Atmospheric Research 304 (2024) 107366

Contents lists available at ScienceDirect

Atmospheric Research

journal homepage: www.elsevier.com/locate/atmosres

# Summer heatwaves in China during 1961–2021: The impact of humidity

Shanjun Cheng [a], Shanshan Wang [b,**], Mingcai Li [c,*], Yongli He [b]

[a] Tianjin Climate Center, Tianjin, China
[b] Key Laboratory for Semi-Arid Climate Change of the Ministry of Education, College of Atmospheric Sciences, Lanzhou University, Lanzhou, China
[c] Tianjin Institute of Meteorological Sciences, Tianjin, China

ARTICLE INFO

*Keywords:*
Heatwave
Wet-bulb temperature
Humidity
China

ABSTRACT

In additon to temperature, heatwaves are also closely related to humidity. In this study, daily wet-bulb temperature was used to define heatwaves (WBHWs) with a unified threshold for more than 2000 meteorological stations throughout China. The climatic averages of summer heatwaves and changes from 1961 to 2021 were investigated. WBHWs primarily occur in three key subregions, namely North China, South China, and Yangtze River valley (YRV). Humidity makes heatwaves in South China more severe, with an average of 25 days per summer. Over the past decades, the frequency and intensity of WBHWs in China considerably increased accompanied by decreasing relative humidity (RH) and increasing temperature. South China experiences the strongest increase in WBHWs, with change rate fivefold higher than the national average. The occurrence of WBHWs in YRV is dominated by temperature, whereas in North and South China it is controlled by RH. The long-term increases in WBHWs for China and its three key subregions are primarily caused by temperature changes, but RH affects WBHWs at interdecadal time scales and generally exerts a negative contribution. The average contribution rates of temperature and RH to the increase in WBHWs in China for the period 1991–2021 are 2.3 days and − 0.6 days. Changes in WBHWs in North China are almost completely controlled by temperature, since the opposite phases of specific humidity and temperature result in a negligible effect of RH. Temperature and RH in other two subregions have substantial positive and negative effects, respectively. The negative effect of RH in South China is mainly attributed to the indirect effect of temperature, while that in YRV, particularly in the lower reaches, is a combination of specific humidity and temperature.

## 1. Introduction

Heatwaves, one of the most severe extreme meteorological disasters, can reduce agricultural production, increase forest and grassland fires, cause a shortage of electricity and water, and affect the incidence of various diseases, directly jeopardizing the growth of the national economy as well as the safety of people's lives and property (Smoyer-Tomic et al., 2003). Currently, 30% of the global population is affected by extreme heatwave events lasting at least 20 days per year (Mora et al., 2017). Along with the climate warming, the frequency, intensity, and duration of global heatwaves have increased significantly (Meehl and Tebaldi, 2004), especially after the 1990s when heatwaves surged (Perkins et al., 2012). Even during the warming hiatus, heatwave events still show a clear increasing trend (Li et al., 2021). However, the variability of heatwaves is highly localized and characteristics based on different indices exhibit discrepancies (Qian et al., 2011; You et al., 2017), with the most pronounced and consistent rises in Europe and eastern China (Perkins et al., 2012).

Since the mid-20th century, heatwaves in China have generally increased and intensified, with obvious interdecadal variability (Sun et al., 2014a; Wei and Chen, 2009, 2011) and regional differences in the long-term trends (Hu et al., 2017). Climate projections suggest that China will experience more severe heatwaves without mitigation efforts (Ma and Yuan, 2023; Wang et al., 2020; Wang and Yan, 2021). The occurrence and increase of heatwaves are especially stronger in highly urbanized and densely populated areas like the Yangtze River valley (YRV) and South China, due to the urban heat island effect (Luo and Lau, 2017, 2018; Yao et al., 2022). Unprecedented heatwave events in these regions, such as 2013 heatwave over a vast area of southern China (Peng, 2014) and the 2017 YRV heatwave (Zhou et al., 2019), have been

* Correspondence to: M. Li, Tianjin Institute of Meteorological Sciences, Tianjin 300074, China.
** Correspondence to: S. Wang, Key Laboratory for Semi-Arid Climate Change of the Ministry of Education, College of Atmospheric Sciences, Lanzhou University, Lanzhou 730000, China.
*E-mail addresses:* wangss@lzu.edu.cn (S. Wang), mingcaili3394@163.com (M. Li).

https://doi.org/10.1016/j.atmosres.2024.107366
Received 9 November 2023; Received in revised form 31 January 2024; Accepted 23 March 2024
Available online 25 March 2024

more frequent for recent 20 years, causing cascading economic losses and a significant impact on mortality (Sun et al., 2014b). In the summer of 2022, the strongest heatwave event since 1961 swept through most parts of eastern China, lasting 79 days and covering more than 5 million square kilometers (Jiang et al., 2023). This high temperature led to the rapid development of meteorological drought in the middle and lower reaches of YRV, Sichuan and Chongqing (Hao et al., 2023). Moreover, Northeast and North China have also frequently affected by heatwaves in recent years. For example, Northeast China experienced multiple consecutive days of high temperatures in late July and early August 2018, with the maximum temperature anomaly exceeding 6 °C (Tao and Zhang, 2019). In June 2023, a record-breaking heatwave event occurred in North China, with daily maximum temperatures exceeding 40 °C at 124 stations (Qian et al., 2024). By the end of the century, the North China Plain may become uninhabitable due to extreme heatwaves (Kang and Eltahir, 2018). Since eastern China is the most economically active region in China, with a high urbanization rate and dense population distribution, the impact of heatwaves here is more severe. Therefore, understanding the characteristics and mechanisms of heatwaves in eastern China is of great significance for regional disaster prevention and mitigation.

Heatwaves are primarily assessed using temperature alone, including extreme temperatures or temperature-based indices. However, it is equally essential to characterize heatwave events by considering humidity, which is directly related to the heat exchange between human body and external environment (Yuan et al., 2020). As humidity increases, the body's ability to dissipate heat will decrease, resulting in an increase in morbidity and mortality of related diseases (Mora et al., 2017). The most deadly heatwaves are more likely to occur in high humidity conditions. The severity of some heatwaves, exemplified by Chicago heatwave in 1995 and China heatwave in 2003, have been strongly amplified by humidity and the percentage of area where humidity amplifies heatwaves expands with increasing warming levels (Russo et al., 2017). Regional humidity varies tremendously in China due to the vast diversity in geographical location and topography (Niu et al., 2020). Therefore, it is more essential to consider both temperature and humidity while studying heatwaves in China. To describe the joint impacts of temperature and humidity, some thermal comfort indices have been proposed and characteristics of heatwaves are explored accordingly. For instance, Luo and Lau (Luo and Lau, 2019a) explored the climatological pattern and long-term trends of summer heat stress occurrences in China during 1979–2014 by using apparent temperature that is derived from temperature and relative humidity (RH). Ding and Qian (2011) investigated geographical patterns and temporal variations of dry and wet heatwave events in China during 1960–2008 with a heat index from the United State National Climatic Data Center. Among the wide variety of composite temperature-humidity indices, wet-bulb temperature (Tw) is an effective and widely used index for characterizing heatwaves due to its clear physical interpretation (Lin and Yuan, 2022; Raymond et al., 2017; Wang et al., 2019; Yu et al., 2021). It is closely linked to the human body's core temperature and can be easily calculated from temperature and relative humidity (RH). Using daily Tw from reanalysis dataset, Yu et al. (2021) investigated the spatial-temporal variation of wet heatwaves in Eurasia for 1979–2017. In their study, East Asia was treated as a whole at a coarser spatial resolution, without considering the regional differences. Ning et al. (2022) investigated the dominant modes of summer Tw in China during 1960–2017 from 746 weather stations.

In this study, we investigated the characteristics of summer heatwaves during 1961–2021 using Tw from 2007 meteorological stations and quantified the contributions of temperature and RH. This study aims to provide insights into regional differences of heatwaves in China from the perspective of humidity, and to quantify the contributions of temperature and RH to heatwave variability in different regions. This is of significance for the risk management of heatwaves and can provide a theoretical basis for the improvement of heatwave prediction in China.

The remainder of this paper is organized in the following manner: The materials and methods are described in Section 2. Section 3 presents the results of our analysis. A conclusion and discussion is provided in Section 4.

## 2. Materials and methods

### 2.1. Data and methods

The data used here are the daily mean temperature, RH, and air pressure of 2479 meteorological stations located throughout China for summer (June–August) of 1961–2021, provided by the China Meteorological Administration. These original data have been made initial quality control by the National Meteorological Information Center of China (Li and Dong, 2009; Li et al., 2004). Based on the quality control, the error values were deleted. Considering the consistency and representativeness of the data, one missing value in the summer of a given year was allowed and all the data for the whole season were set as missing values if two daily missing value existed. Then the station was removed if there are more than four summers with more than two missing days. 2007 out of 2479 stations were selected under this condition. Among the 2007 stations, 24.8% of stations have no missing data and 40.0% only have one missing year in the 61-year period. In view of the fact that missing data can constrain the definition of heatwaves, missing values for one day duration are interpolated with the average values of the day before and the day after, while missing values lasting two days or more are interpolated with the climatological period of 1961–1990.

Daily Tw (units: °C) was calculated from daily temperature (T; units: °C) and RH (units: %) values using the following formula (Stull, 2011).

$$T_w = T \times atan\left[A(RH+B)^{\frac{1}{2}}\right] + \mathrm{atan}(T+RH) - \mathrm{atan}(\mathrm{RH}-\mathrm{C}) + \mathrm{D}(RH)^{\frac{3}{2}} \times \mathrm{atan}(E \times RH) - F \quad (1)$$

where A, B, C, D, E, F are constants (A = 0.152, B = 8.314, C = 1.676, D = 0.004, E = 0.023, F = 4.686), obtained by fitting functions (Stull, 2011). According to this equation, Tw is positively related to temperature and RH. It means for a given temperature, the higher the RH, the higher the Tw. That is the reason why wet conditions results in less human thermal comfort. However, temperature exhibits a significant negative correlation with RH (correlation coefficient: −0.92), implying that the highest Tw does not occur at the maximum value of temperature or RH (Fig. S1). According to the equation of RH, RH is a function of specific humidity, air pressure and temperature.

$$RH = \frac{e}{e_s} \times 100 = \frac{q \times P}{0.622 \times e_s} \times 100 \quad (2)$$

$$e_s = 6.1078 \times exp\left(\frac{17.269 \times T}{T + 273.15 - 35.86}\right) \quad (3)$$

where $e$, $e_s$ and $P$ are water vapor pressure, saturated water vapor pressure, and air pressure (units: hPa), $q$ is specific humidity (units: g/g).

It should be noted that the equation of Tw is an empirical fit, which is not valid for situations having both low humidity and cold temperature (such as high altitudes). Wet bulb globe temperature is a more comprehensive index for defining heatwaves, combining temperature, humidity and radiation (Heo et al., 2019). The number of stations with radiation data (about 50) is far fewer than those for temperature and humidity in China, limiting the use of this index. Thirty-two stations containing simultaneously temperature, humidity, and radiation observations were selected to evaluate the relationship between Tw and wet bulb globe temperature. The monthly and inter-annual variations of the two indices in China are highly consistent, and only two stations on the Tibetan Plateau exhibit correlation coefficients less than 0.7

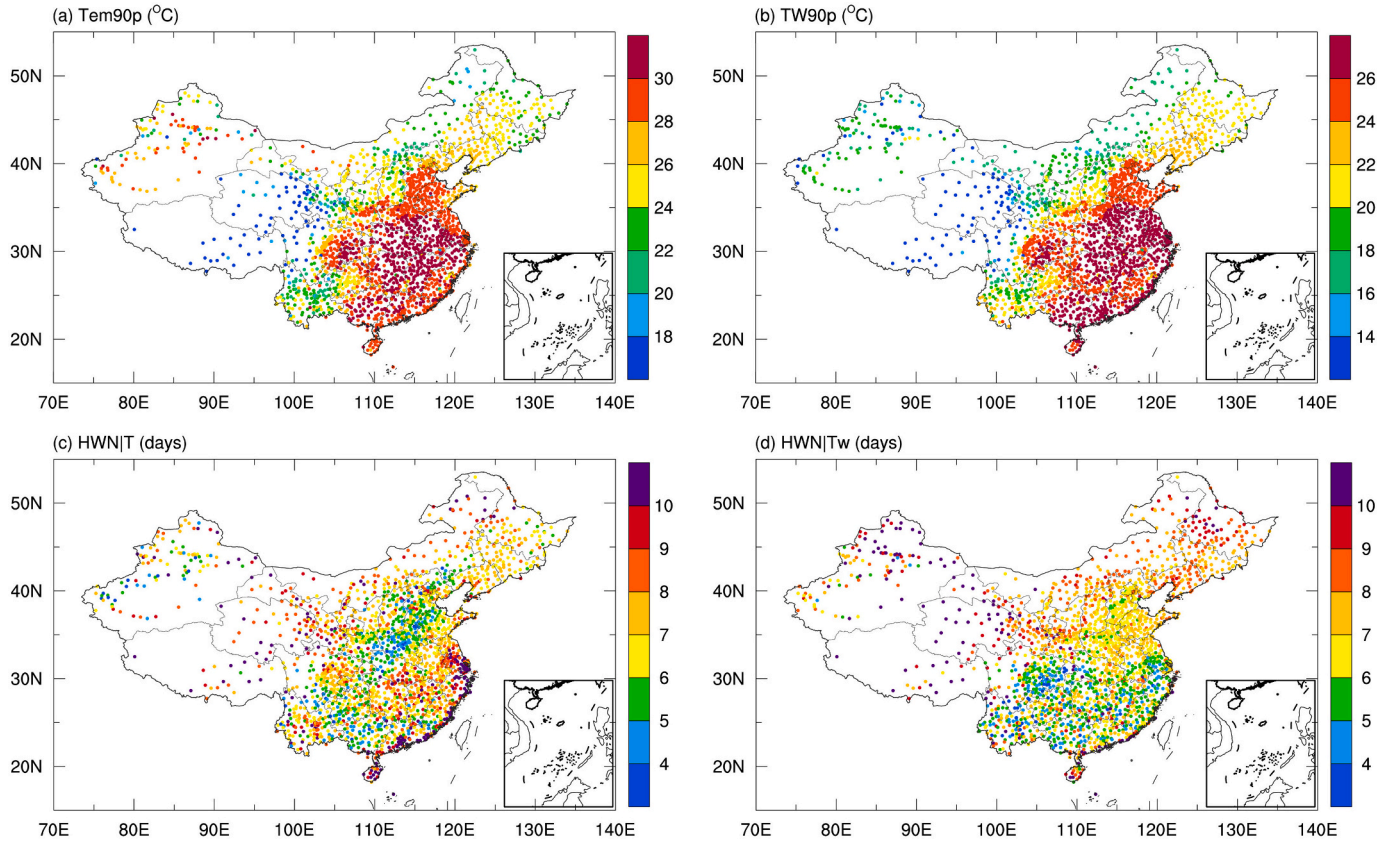


**Fig. 1.** The 90th percentile of daily (a) temperature and (b) wet-bulb temperature (Tw) during summer for the period 1961–1990 at each station in China. Summer mean HWN for the period 1961–2021 based on (c) temperature and (d) Tw.

(Fig. S2). Besides, Tw shows a remarkable resemblance with apparent temperature spatially and temporally, with correlation coefficients larger than 0.7 in most areas of eastern China (Figs. S3 and S4). This suggests that Tw can be used to characterize heatwaves in eastern China.

Probability density function was adopted to describe the variable distribution. It is a function that specifies the likelihood of a random variable falling within a particular range of values in the sample space (Kumaraswamy, 1980). Besides, regression analysis and correlation analysis were used in this study to calculate linear trends and linear correlation coefficients. The statistical significance of trends and correlation coefficients were determined according to the two-tailed probability of the Student's *t*-test.

### 2.2. Identification of heatwaves

Heatwaves are defined as prolonged periods of excessive heat, measured by a threshold (Perkins and Alexander, 2013). In previous studies, the thresholds for defining heatwaves based on Tw are usually localized, i.e., different thresholds for different regions (Raymond et al., 2017; Wang et al., 2019; Yu et al., 2021). Due to the large geographic extent of China, the climatic characteristics of different regions vary greatly, with cold climatic environments in some areas. Localized thresholds may yield heatwave events with relative low temperatures, though the temperatures are extremes for the certain region. As shown in Fig. 1a and b, the 90th percentile of daily summer temperature and Tw varies dramatically among stations in China, with temperature ranging from 7.4 °C on the Qinghai-Tibet Plateau to 34.8 °C in southern China, and Tw ranging from 4.9 °C to 27.6 °C. Using this localized threshold and a duration of more than 3 days as the definition of heatwaves, the total number of heatwave days per summer (HWN) for the period 1961–2021 is shown in Fig. 1c and d. It demonstrates that heatwaves based on temperature are concentrated along the eastern coastal regions and on the Tibetan Plateau. Heatwaves based on Tw (WBHWs) are more frequently occurred in northwestern and northeastern China, with more than 10 days per summer, while in southern China they are less than 4 days. This is unreasonable. In fact, the definition based on localized threshold refers to abnormal temperatures, instead of heatwave events, which should be accompanied by high temperatures. Thus, the threshold in this study is unified as the 90th percentile of daily summer Tw for all meteorological station in China for the base period 1961–1990, which is 25.9 °C. A WBHW event was defined as three or more consecutive days during summer with a daily Tw above the threshold. Meanwhile, a heatwave event based on temperature (THW) was defined the same as WBHW, but using daily temperature with a threshold of 29.2 °C.

The total number of heatwave days per summer (HWN) was adopted to characterize heatwaves in this study. HWN shows a remarkable resemblance with other three indices, representing the duration, intensity of heatwaves and stations affected by heatwaves (See supplement for details).

### 2.3. Contributions of temperature and RH to Tw and WBHWs

According to Yu et al. (2021), the equation for the quantitative effects of temperature and RH variations on Tw is as follows.

$$\Delta T_w = \Delta T \frac{\partial T_w}{\partial T} + \Delta RH \frac{\partial T_w}{\partial RH} + R \quad (4)$$

where ΔT and ΔRH are the trends of temperature and RH from 1961 to 2021. ∂Tw/∂T (°C/°C) and ∂Tw/∂RH (°C/%) are the partial differentiation of Tw with respect to temperature and RH. R is a residual representing 2nd and higher order terms. A detailed description can be found in Yu et al. (2021).

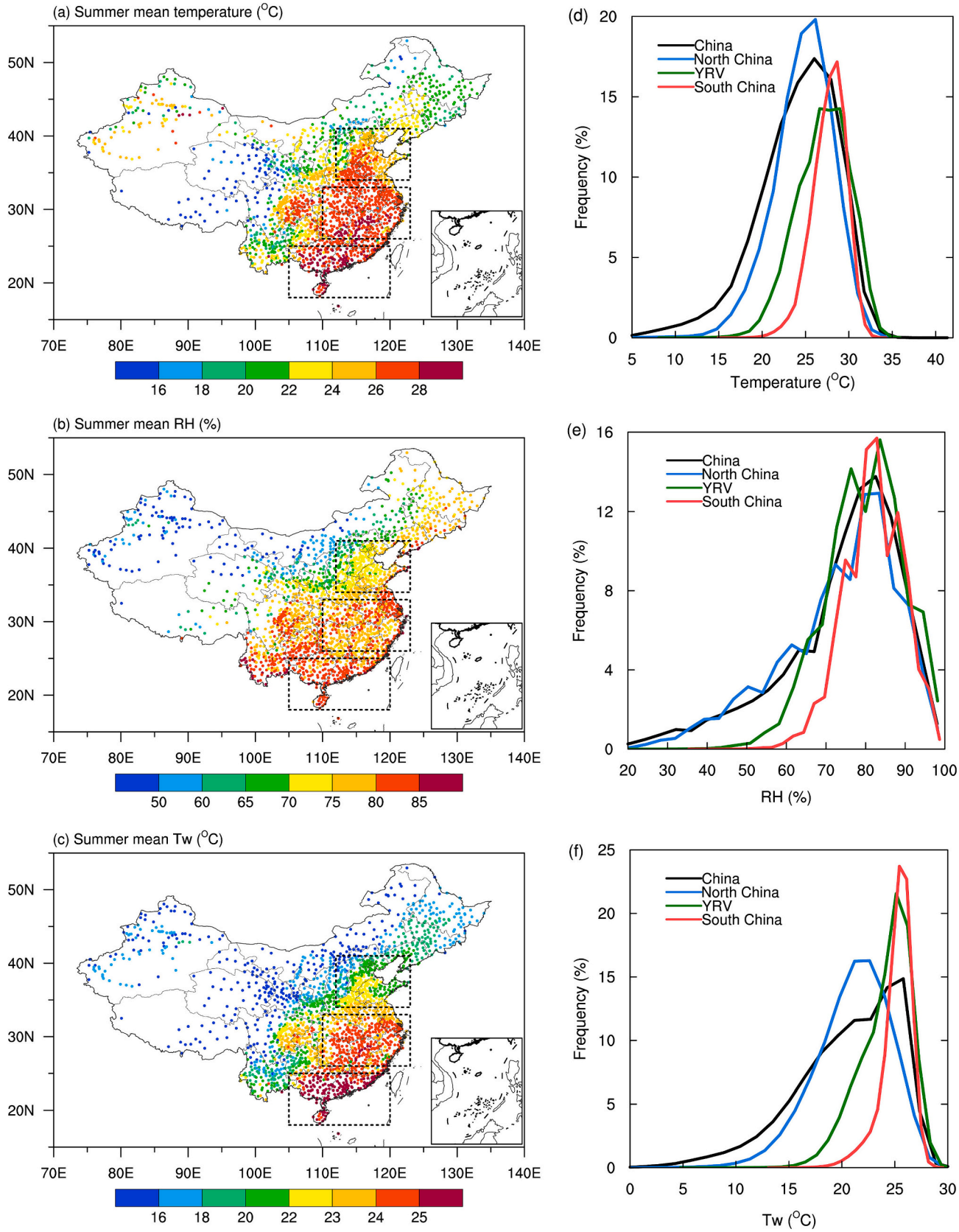


**Fig. 2.** (Left) Summer mean (a) temperature, (b) relative humidity (RH) and (c) Tw for the period 1961–2021. (Right) Probability density functions of (d) temperature, (e) RH and (f) Tw in China and its three subregions. Dashed boxes from north to south denote North China, the Yangtze River valley (YRV), and South China.

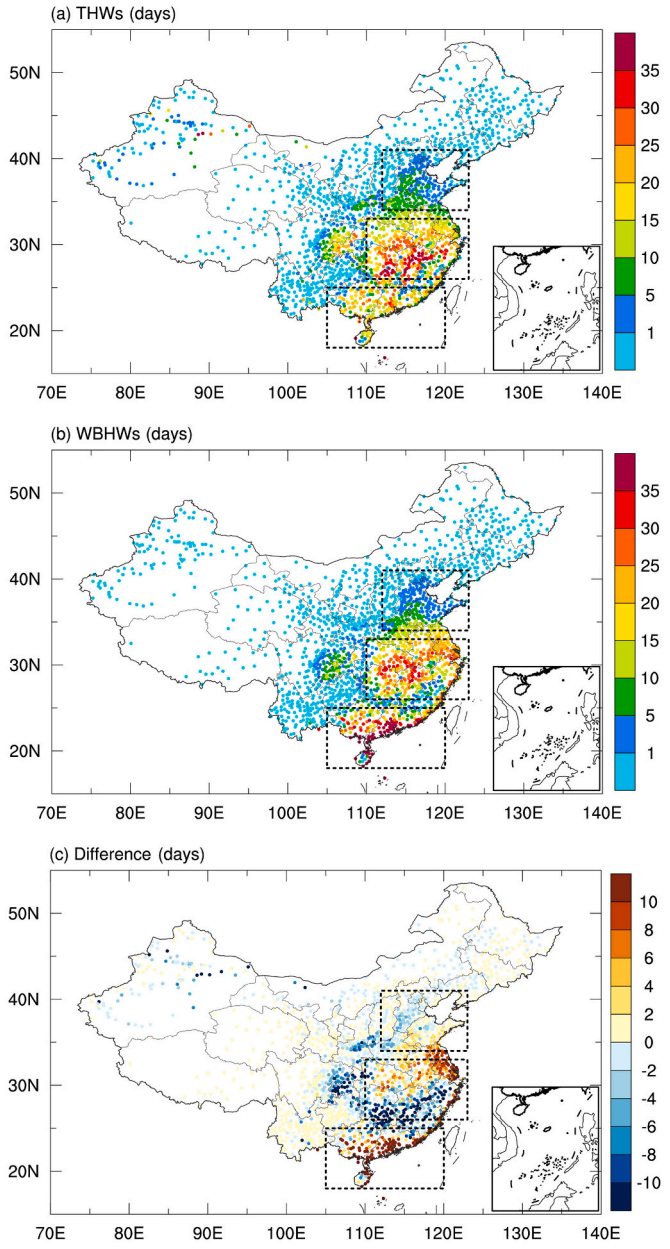


**Fig. 3.** Summer mean HWN of (a) THWs, (b) WBHWs for the period 1961–2021 and (c) the difference in the two indices (WBHWs minus THWs). Dashed boxes from north to south denote North China, YRV, and South China, respectively.

Since heatwaves are defined subjectively without a certain equation, the contributions of changes in temperature and RH to the change in WBHWs were evaluated by two additional computations of Tw with reference to Jones' method (Jones et al., 2015). The two computations are also based on Eq. (1) but using the climatological average of RH (temperature) over the whole period for all years, which means the signal of RH (temperature) change is removed from Tw. On this basis, HWN was calculated based on the two computations, which can be roughly determined as the HWN component caused by temperature or RH. Therefore, anomalies of the temperature-caused or RH-caused HWN component in each year are defined as the contribution rate of temperature or RH to WBHWs. Similarly, four additional Tw were calculated using a given variable and climatological average of all other variables, and thus the WBHWs were counted. These components can be treated as contributions of temperature, specific humidity, and air pressure. Contributions of temperature consists of direct effect caused by changing temperature and constant RH, as well as indirect effect by influencing RH. The sum of direct and indirect effects is the total effect of temperature. Theoretically, the sum of indirect effect of temperature, effect of specific humidity, and effect of air pressure equals that of RH.

## 3. Results

### 3.1. Climatological characteristics of heatwaves in China

Fig. 2 depicts the spatial distributions of temperature, RH and Tw, which shows that warm temperatures and high RH mainly exit in southern China. According to the probability density functions, the most frequent daily temperature in China over the past 61 years is around 26 °C (frequency: 17.4%), and 46.9% ranges from 26 °C to 42.3 °C. More than half of the days have a RH greater than 78%, with a peak value of around 80%. The hot and humid environment in southern China leads to high Tw, with the maximum in Guangdong and Guangxi provinces. Climatological average of HWN for THWs is shown in Fig. 3a. Except for a few stations in Xinjiang, heatwaves are mainly observed in eastern China that is east of 100°E and south of 40°N, while the summer mean HWN in other regions is less than 1 day. Eastern China was divided into three subregions, i.e., North China (112–123°E, 34–41°N), YRV (110–123°E, 26–33°N) and South China (105–120°E, 18–25°N), with the ranges depicted in Fig. 3. These three areas are densely populated areas and encompass lots of big and medium-sized cities. YRV is the subregion with the highest concentration of THWs, followed by South China and North China. The mean HWN in the three subregions are 3.7, 19.2 and 15.1 days, respectively (Table 1). Fig. 3b displays the distribution of HWN for WBHWs, with high incidence also appearing in eastern China. However, the HWN in the coastal areas of South China is comparable to or even higher than that in YRV due to the warm and wet condition, which are distinct from the THWs. Generally, WBHWs are more severe than THWs in South China and Jiangsu, while THWs are more intense in the southern part of YRV (Fig. 3c). The mean WNHWs in North China, YRV and South China are 3.6, 18.6 and 25.0 days, respectively (Table 1). The WBHWs in South China are 9.9 days longer than THWs, indicating the critical role of humidity on heatwaves in this region.

The regional differences in heatwaves are derived from the relevant variables. As shown in Fig. 2d, the most frequent temperatures in YRV and South China (around 29 °C) are identical and larger than that in North China (around 26 °C). Temperature in YRV has a wider range, with the 5th and 95th percentiles being 21.7 °C and 31.6 °C (24.2 °C and 30.5 °C in South China; Table 1). The extension of the right tail in YRV results in the more frequent extremely high temperatures and THWs. Despite the larger climatology of temperature in South China, the HWN

**Table 1**
Climatological averages and extreme values (5th and 95th percentiles) of temperature, RH, Tw and HWN in China and its three subregions during 1961–2021.

| | Temperature (°C) | | | RH (%) | | | Tw (°C) | | | HWN (days) | |
|---|---|---|---|---|---|---|---|---|---|---|---|
| Index | 5th | AVG | 95th | 5th | AVG | 95th | 5th | AVG | 95th | THWs | WBHWs |
| China | 15.4 | 24.1 | 30.3 | 41 | 73.9 | 93 | 11.2 | 20.5 | 26.6 | 7.4 | 7.4 |
| North China | 18.7 | 24.7 | 29.8 | 44 | 73.0 | 92 | 14.7 | 21.0 | 26.1 | 3.7 | 3.6 |
| YRV | 21.7 | 27.0 | 31.6 | 63 | 79.7 | 95 | 19.6 | 24.1 | 27.3 | 19.2 | 18.6 |
| South China | 24.2 | 27.7 | 30.5 | 69 | 81.9 | 94 | 22.2 | 25.2 | 27.0 | 15.1 | 25.0 |

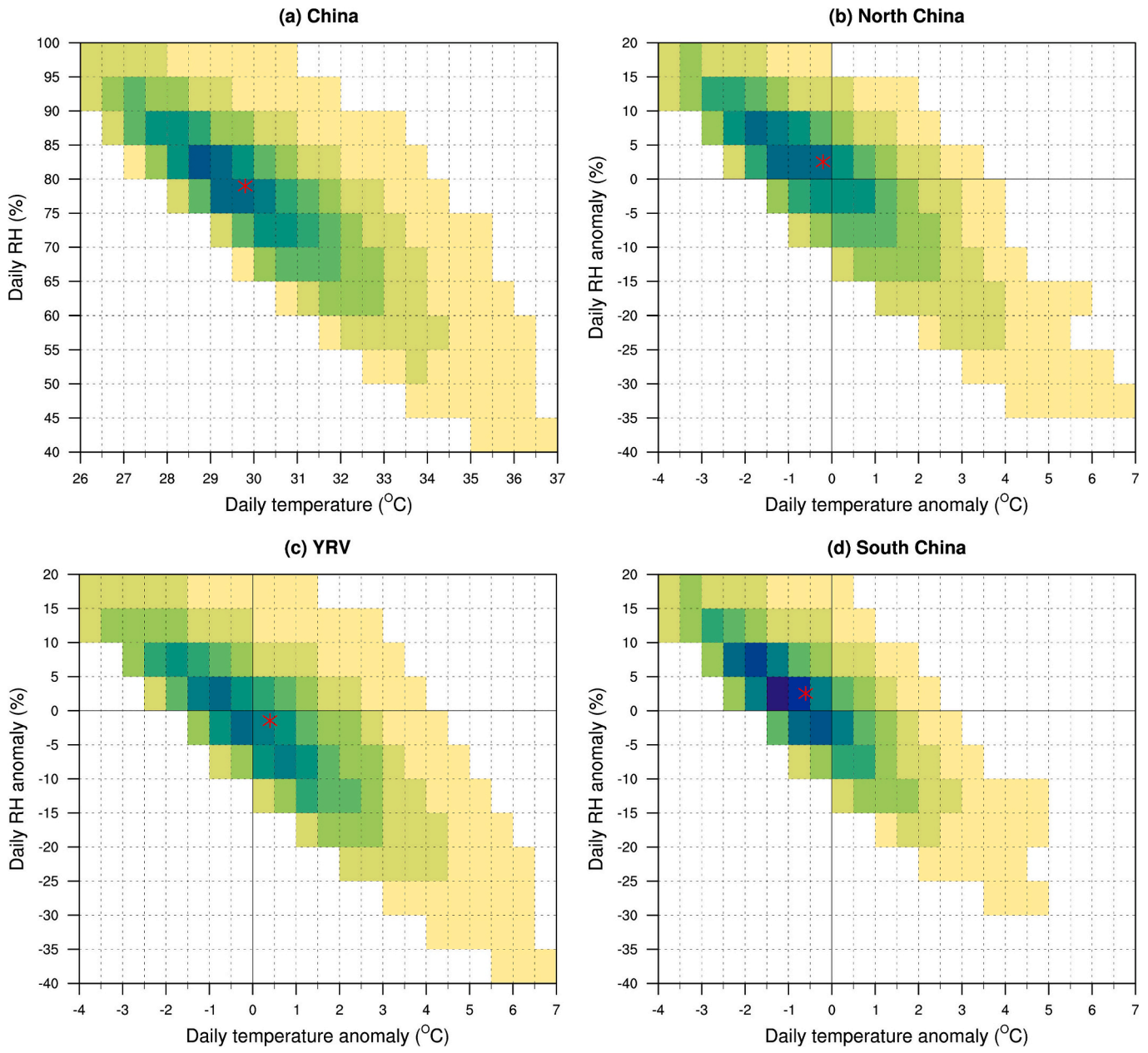


**Fig. 4.** Percentages of HWN for WBHWs as a function of daily temperature (or temperature anomaly) and RH (or RH anomaly) in China and its three subregions. The colored boxes represent percentages of heatwave days. The anomalies of temperature and RH in subregions are relative to the average of China. The markers are the medians of daily temperature and RH.

in YRV is 4.1 days longer than that in South China (Table 1). This result indicates that the extremes and the average values of temperature do not exactly coincide. Compared with temperature, the probability density function of RH in the three subregions presents more resemblance, with the most frequent RH of roughly 83% and more consistent curves after the wave peak (Fig. 2e). The more concentrated range in South China results in a larger climatology of RH (Table 1). The probability density functions of Tw are similar to those of temperature, except coincident upper thresholds in the three subregions (Fig. 2f). As a result of the higher lower threshold (22.2 °C), South China has the largest climatology of Tw and WBHWs. Additionally, the curves for temperature and Tw are smoother than those for RH, indicating a better continuity of temperature indices.

Since the maximum Tw does not coincide with those of temperature or RH, WBHWs are more prevalent at a certain temperature and RH value rather than the hottest or wettest conditions. The relationship between percentages of WBHWs versus daily temperature (or temperature anomaly) and RH (or RH anomaly) is depicted in Fig. 4. The anomalies of temperature and RH in the subregions are relative to the national average. It indicates that WBHWs in all three subregions are more likely to occur close to the medians of temperature and RH and extend to the second and fourth quadrants. Among the three subregions, the conditions for the occurrence of WBHWs are more concentrated in South China, where more than 20% of WBHWs occur at RH of 80–85% and temperature of 28.5–29 °C. This is because of the largest concentration of Tw in South China. Due to the varied probability density functions of climate variables, the medians of temperature and RH as well as the climatic conditions for the high-occurrence of WBHWs are not in agreement in the three subregions, with higher RH in North and South China and higher temperature in YRV. This suggests, to some extent, the critical role of temperature for WBHWs in YRV, and the importance of RH in North and South China.

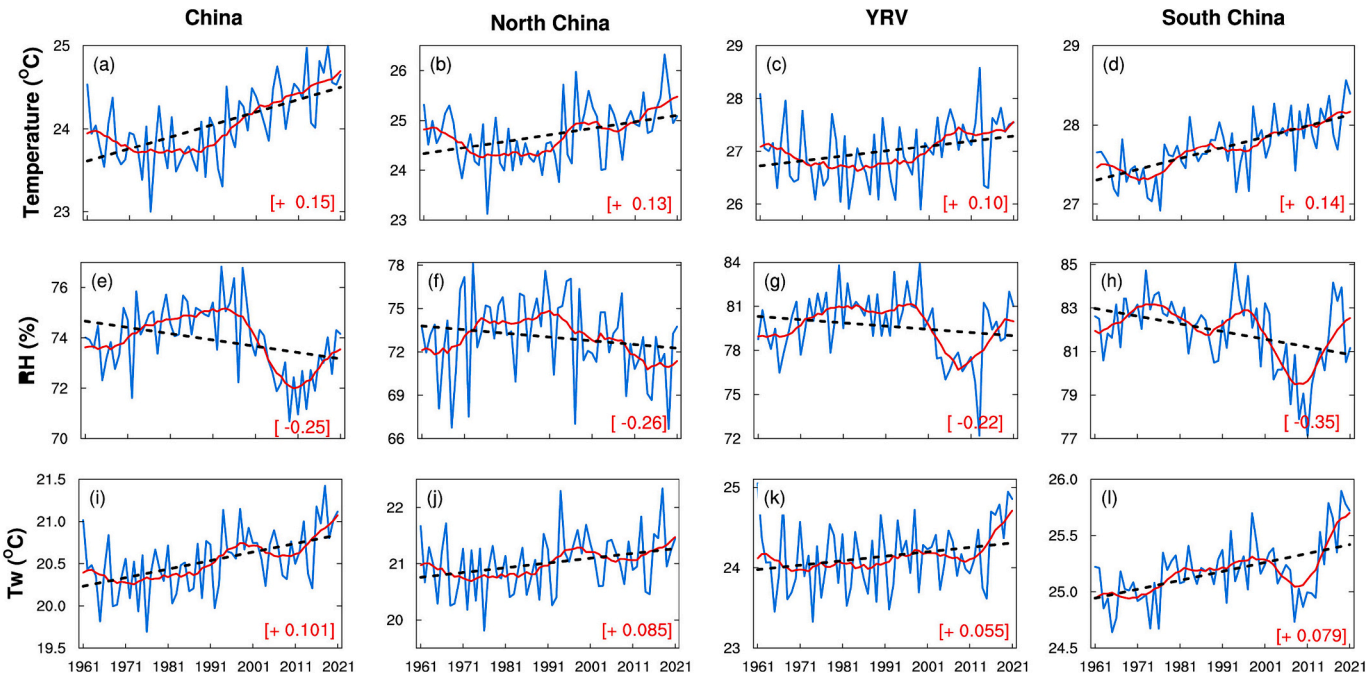


**Fig. 5.** Time series of regional temperature, RH, and Tw in China and its three subregions during 1961–2021. The red lines are the 11-year moving average, and black dashed lines are the linear trends. The numbers in square bracket denote the corresponding trends in per decade. (For interpretation of the references to colour in this figure legend, the reader is referred to the web version of this article.)

### 3.2. Changes of heatwaves in China

The time series and trends of summer mean temperature, RH and Tw over China from 1961 to 2021 are plotted in Figs. 5 and 6. Most land areas have warmed by 0.5 to 3 °C, with the warmest regions located over northern China (Fig. 6a). Rapid warming in China and its three subregions began in the late 1970s (Fig. 5). The long-term variability of RH over China exhibits decreasing trends, with rates ranging from −0.22 to −0.35%/decade for the three subregions. 54.3% of China reveals a significant trend ($p = 0.1$) and mostly is negative (97.5%) except for a few positive stations in Central China. The decreasing RH is due to the fact that the increase rate of temperature exceeds the rate of specific humidity, resulting in a more prominent increase in saturated water vapor pressure than water vapor pressure (Figs. S5 and S6). The most notable decrease is in Beijing-Tianjin-Hebei region and the eastern coastal regions, which are highly urbanized. This may be related to the urban dry island effect, as characterized by reduced humidity and increased vapor pressure deficit in the urban core area (Hao et al., 2018; Luo and Lau, 2019b). Three distinct periods exist for RH variability over China: an increasing period from 1961 to 1991, a subsequent reduced period until 2011, and a second increasing period in the last decade. The period in YRV coincides with that in China, but RH in North China decreases continuously since the early 1990s and decadal fluctuations of RH in South China exist from 1961 to 1991. Affected by temperature and RH, Tw in China and its three subregions also exhibits increasing trends, but the warming rates are less than those of temperature due to the decreasing RH. As shown in Fig. 6c, the largest increase is mainly in northeast China, as it is one of the most significant warming regions and also characterized by increasing trend in RH. The temporal variation of Tw is basically consistent with temperature except that Tw decreases in the 2000s due to the influence of RH. The correlation coefficients between Tw and temperature in China and its three subregions are all larger than 0.7. The upward trends of Tw in North China, YRV, and South China are 0.085, 0.055 and 0.079 °C/decade, respectively.

Accompanied by the changes in temperature and Tw, the summer heatwaves also exhibit increasing trends (see Table 2 and Fig. 7). Fig. 7 displays the time series of HWN for THWs and WBHWs in China during 1961–2021. To emphasize the decadal characteristics, the 11-year moving average is shown. The nationwide THWs and WBHWs rise by 0.65 and 0.45 days/decade for the whole study period, respectively. The two time series are remarkably consistent before the late 1990s, basically showing a decrease followed by an increase. The correlation coefficients between THWs and WBHWs are 0.81 during this time period. Subsequently, THWs continue to increase and enhance, with the average HWN for 2001–2010 and 2011–2021 increasing by 2.6 days and 3.6 days compared to the 1961–1990 average. WBHWs reduce in the 2000s and rise in the 2010s due to the changes in RH. The average HWN for 2001–2010 is essentially comparable to the 1961–1990 average. The rapid increase in heatwaves since the 2010s is closely related to the phase changes of El Niño–Southern Oscillation and Indian Ocean Dipole (Wei et al., 2023). In addation, HWN for the two types of heatwaves shows a remarkable resemblance with other three indices, representing the duration, intensity, and stations of heatwaves (Figs. S7 and S8). The correlation coefficients with each other all exceed 0.9.

Fig. 8 depicts the spatial distributions of the trends in HWN across China. Significant trends ($p = 0.1$) for THWs and WBHWs are observed for 33.5% and 21.6% of the stations where heatwaves occur. They are dominated by increasing trends at proportions of 93.8% and 92.6%, respectively. The most prominent trends in THWs mainly occur in coastal areas of South China and YRV. WBHWs in South China also exhibit more significant increasing trends than other areas, with a rate of more than 5 days/decade. It should be noted that these areas do not coincide with the areas with the largest increasing temperature and Tw, indicating that the changes in extreme temperature is not entirely dependent on the average temperature. The most pronounced differences in trends of WBHWs and THWs are located in the west-central part of YRV, where WBHWs exhibit a considerable increase whereas THW trends are not significant at most stations. In addition, the trend of THWs in North China is also slightly larger than that of WBHWs. In terms of regional averages, South China has a substantially higher increase in heatwaves than the other two subregions, with trend rates of 2.57 and 2.44 days/decade for THWs and WBHWs, respectively. The time series of WBHWs in the three subregions are generally consistent (Fig. 8c), with an overall “increasing-decreasing-increasing” pattern over the last

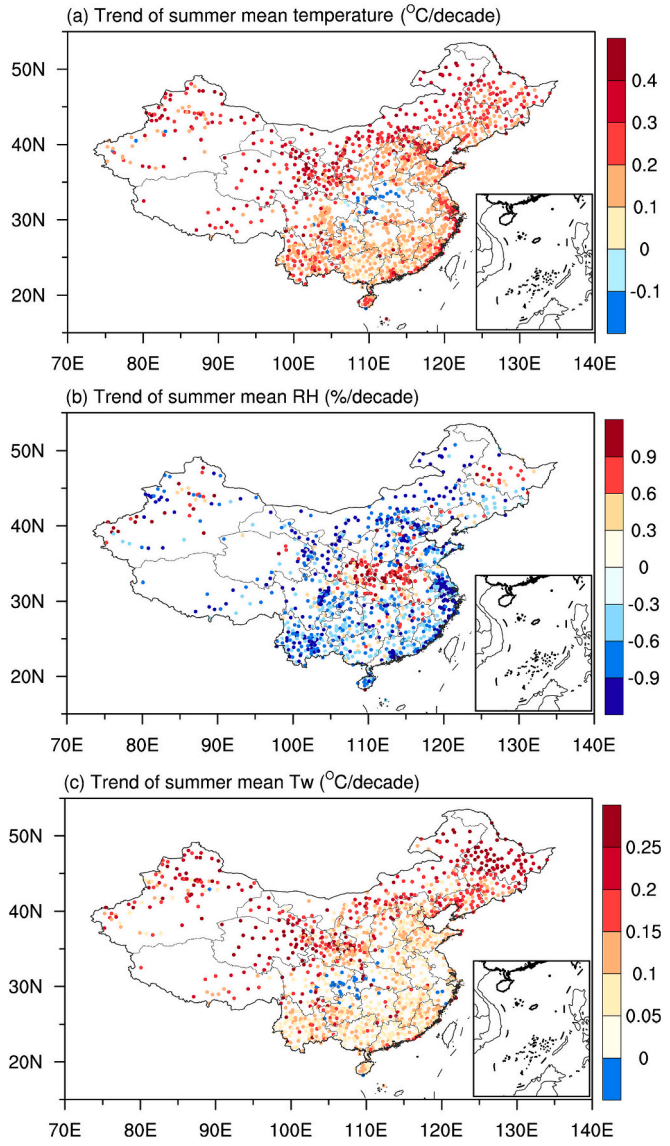


**Fig. 6.** Trends of summer mean (a) temperature, (b) RH, and (c) Tw over the period 1961–2021. Only stations with significant trend at the 0.1 level are shown.

**Table 2**
Trends of heatwave indices and relevant variables in China and its three subregions during 1961–2021. Bold font denotes significance at the 0.1 level.

| Index (units/decade) | China | North China | YRV | South China |
|---|---|---|---|---|
| Temperature (°C) | **0.15** | **0.13** | **0.095** | **0.14** |
| RH (%) | **−0.25** | −0.26 | −0.22 | **−0.35** |
| Tw (°C) | **0.10** | **0.085** | **0.055** | **0.079** |
| THWs (days) | **0.65** | **0.42** | **0.99** | **2.57** |
| WBHWs (days) | **0.45** | 0.28 | 0.64 | **2.44** |
| T-caused (days) | **0.70** | **0.51** | **1.10** | **2.70** |
| RH-caused (days) | −0.044 | **0.062** | −0.040 | **−0.72** |

three decades. In contrast, the variation of THWs has obvious regional differences, with North China showing a decrease in the 2000s and basically consistent with WBHWs throughout the time period, the YRV region increasing from the mid-1990s to the end of the 2000s and then entering in a stable phase, and South China displaying a continuous increasing trend since the early 1970s. Moreover, the WBHWs are significantly larger than THWs in South China throughout the study period, highlighting the important role of RH on heatwaves in this region.

### 3.3. Effects of temperature and RH to Tw and WBHWs

To disentangle the effects of temperature and humidity on extreme Tw, Raymond et al. (2017) defined a index as the ratio of standardized temperature and standardized specific humidity. Depending on the index, an extreme Tw day can be classified as temperature-dominated or humidity-dominated. As the temperature threshold in our definition is uniform across all the stations, the daily temperatures during WBHWs are larger than the climatological average at most stations, resulting in the index greater than 1. In fact, THWs and WBHWs usually co-occur in eastern China, which means daily temperature is higher than the 90th percentile. Therefore, the percentages of high temperature and RH during WBHWs were calculated, where high temperature refers to the 90th percentile and high RH refers to the mean RH for all summer days during 1961–2021 over the whole China. Fig. 9b shows that the proportion of high RH exceeds 60% or even 90% at most stations in North and South China. It means that WBHWs in this region are more likely to occur under wet conditions, highlighting the dominant role of humidity on the occurrence of WBHWs. This indicates, to some extent, that WBHWs are RH-dominated in North and South China. Conversely, the proportion of high RH in YRV is relatively lower than that in the other two regions, but the proportion of extreme high temperatures surpasses 70% at most stations. This indicates that WBHWs in YRV occur mainly at high temperature conditions, highlighting the critical role of temperature. In other words, WBHWs are temperature-dominated in YRV. In addation to the high values of temperature and RH, composite anomalies of daily temperature and RH during WBHWs are also conducted (Fig. 9c, d), which represents the average deviation from climatic conditions. To be consistency with the unified threshold in the definition of heatwaves, the anomalies are relative to all summer days during 1961–2021 over the whole China. During WBHWs, coherent positive temperature anomalies are seen over all the subregions, and the anomalies in YRV are stronger than those in North China and South China. RH exhibits positive anomalies during most of WBHWs, with large values concentrated in North and South China. Composite anomalies for different subperiods yield identical conclusions (Fig. S9), demonstrating the stability of the results. The anomalies are consistent with the conclusions exhibited by the two percentages shown in Fig. 9a, b.

$\partial Tw/\partial T$ and $\partial Tw/\partial RH$ can represent the sensitivity of Tw to temperature and RH. As shown in Fig. 10a, a 1 °C warming leads to a 0.8–1.0 °C increase in Tw, with large values located in the southwest, southern China, and YRV. This implies that the Tw in southeast China is more sensitive to changes in temperature. A 1% increase in RH leads to a 0.1–0.2 °C increase in Tw, and the highly sensitive areas are mainly observed in Xinjiang and parts of YRV. In general, the distributions of $\partial Tw/\partial T$ and $\partial Tw/\partial RH$ are in agreement with that of climatological mean RH and temperature in Fig. 2. This is because Tw is highly positively correlated with temperature and RH, then a lesser change in RH (temperature) can lead to a larger change in Tw in the high temperature (RH) condition, indicating that Tw is more sensitive to changes in RH (temperature). Trend$T^*\partial Tw/\partial T$ and trend$RH^*\partial Tw/\partial RH$ were then calculated in accordance with Eq. (4) to quantitatively assess the effects of changes in temperature and RH on Tw. The spatial distributions are almost identical to the trends in temperature and RH (Fig. 10c, d), as the spatial variations in the sensitivity of Tw are not obvious and cannot alter the patterns of temperature and RH trends. Overall, the change in temperature contributes positively to Tw while RH has a negative impact in most parts of China. The increase or decrease of Tw depends on the contributions of temperature and RH. In 2011–2021, the effects of temperature and RH are positive in all the three subregions, resulting in a significant increase in Tw. In 2001–2010, temperature contributes positively and RH negatively, while the changes in Tw vary among the three subregions. The contribution of temperature exceeds that of RH in

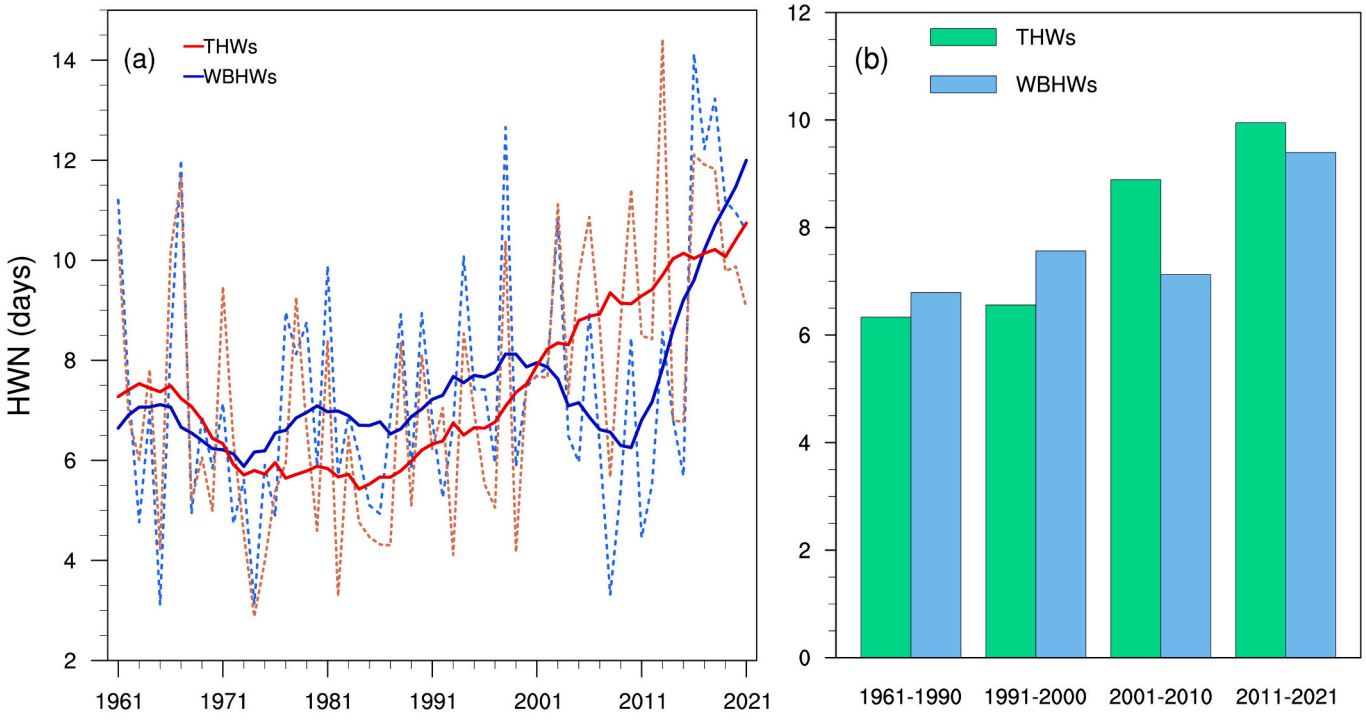


**Fig. 7.** (a) Time series of HWN in China during 1961–2021 for THWs and WBHWs. The solid lines are the 11-year moving average. (b) Average of HWN for the periods 1961–1990, 1991–2000, 2001–2010 and 2011–2021.

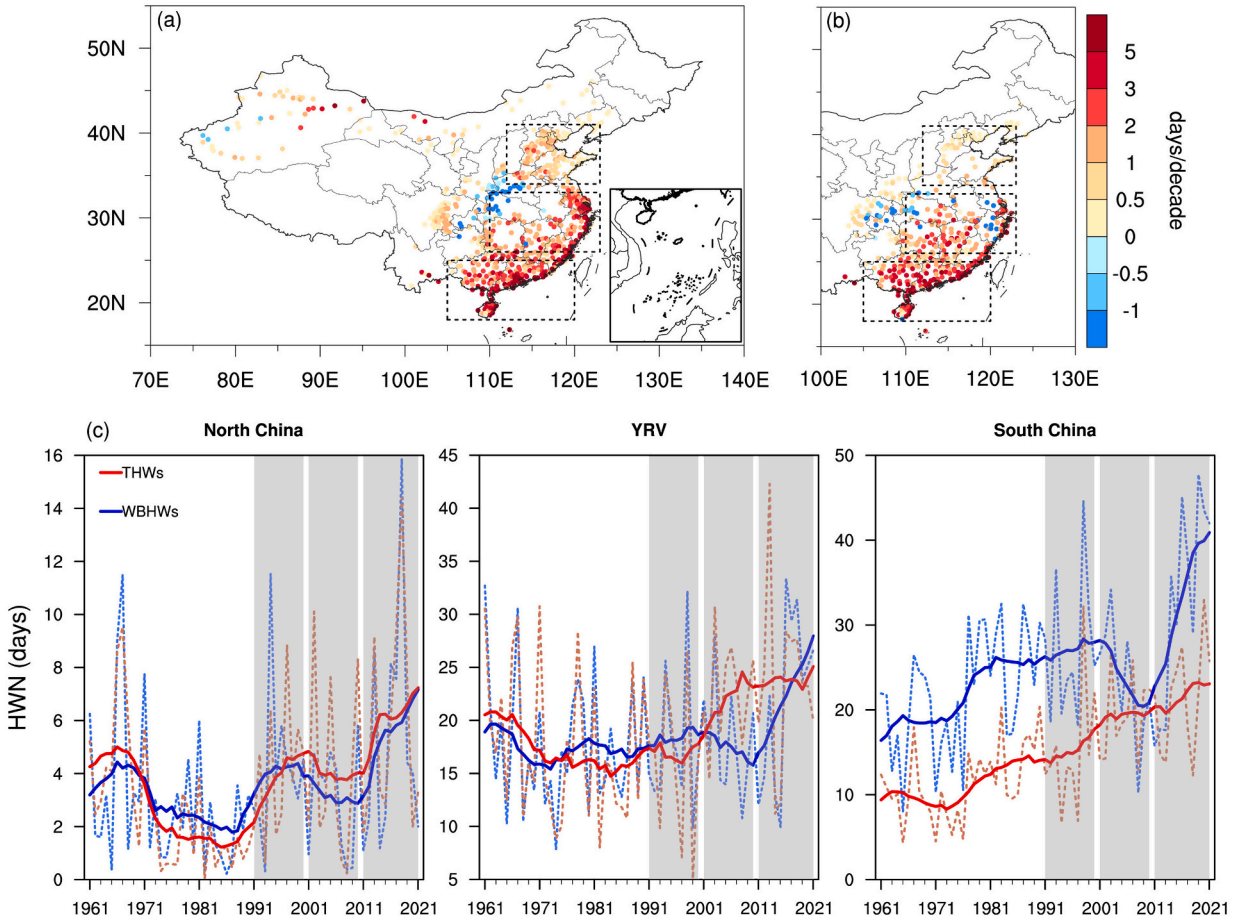


**Fig. 8.** Trends of HWN over the period 1961–2021 for (a) THWs and (b) WBHWs. Only stations with significant trend at the 0.1 level are shown. (c) Same as Fig. 7a, but for the three subregions.

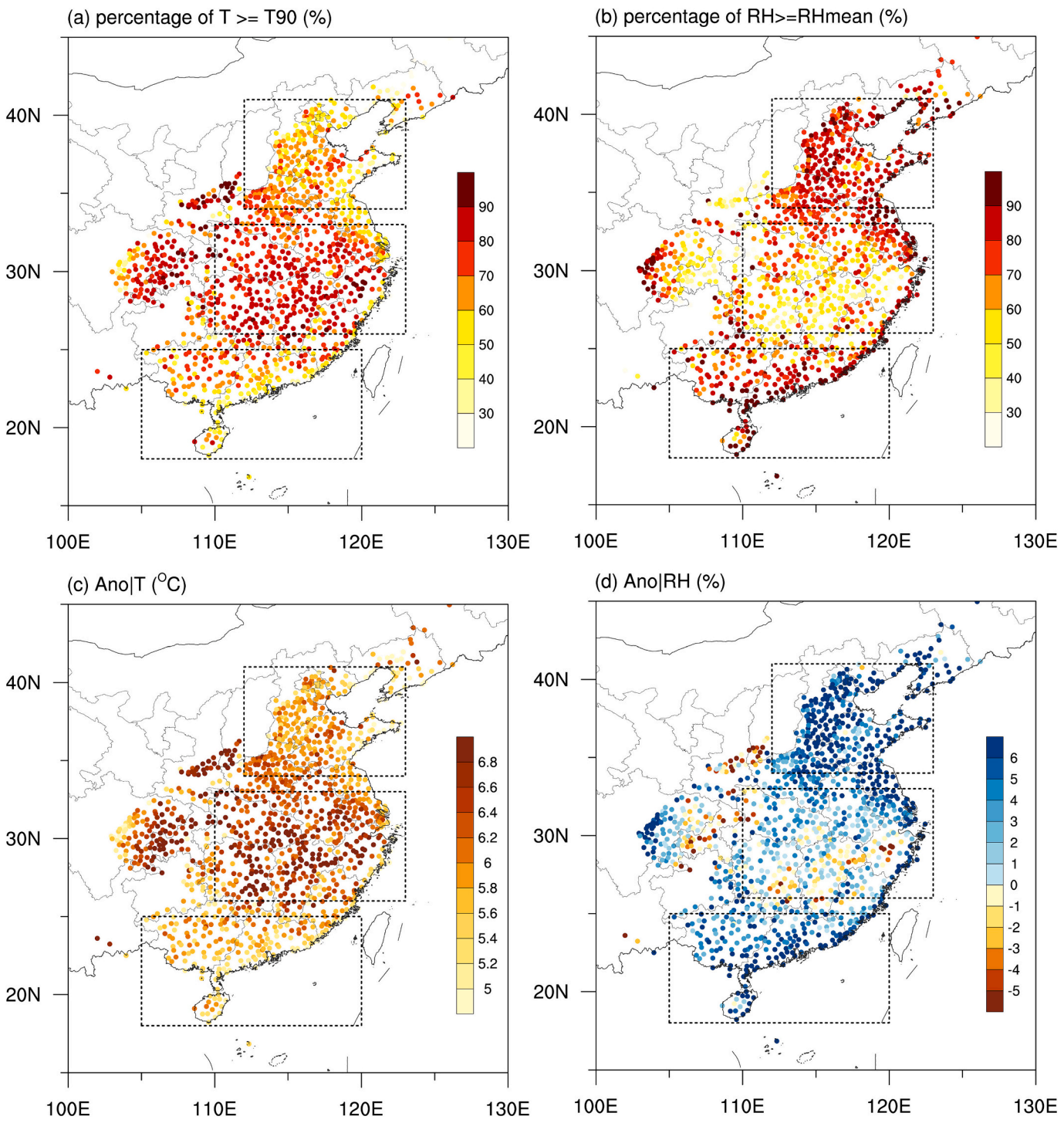


**Fig. 9.** Percentages of (a) temperature ≥ T90 and (b) RH ≥ RHmean during WBHWs for 1961–2021, where RHmean, T90 are the mean RH and 90th percentile of temperature for all summer days during 1961–2021 over the whole China. Composite anomalies of daily (c) temperature and (d) RH during WBHWs for 1961–2021. The anomalies are relative to all summer days during 1961–2021 over the whole China.

North China, leading to an increase in Tw, while RH dominates the decrease of Tw in YRV and South China (Fig. S10). In addition, the trends of the two additional Tw, as mentioned in Section 2.3, closely correspond to the results for trendT*$\partial$Tw/$\partial$T and trendRH*$\partial$Tw/$\partial$RH (Fig. S11).

Fig. 11 displays the regional temperature-caused and RH-caused WBHWs in China and its three subregions during 1961–2021. For comparison, the time series of HWN for WBHWs are also given in the figure. When compared to HWN of WBHWs, the long-term variability of the RH-caused component in China is not significant, despite a declining tendency over the entire time span at a rate of −0.18 days/decade. However, it correlates strongly with the HWN at decadal time scales. In contrast to the RH-caused component, the time series of temperature-caused component has a subtle decadal fluctuation and observable long-term trend. The rate is 0.69 days/decade and significantly exceeds the 95% confidence level. Notably, it slightly declines prior to 1987 but has been dramatically rising since then at a rate of 1.5 days/decade. This significant decreasing trend coincides with climate warming starting

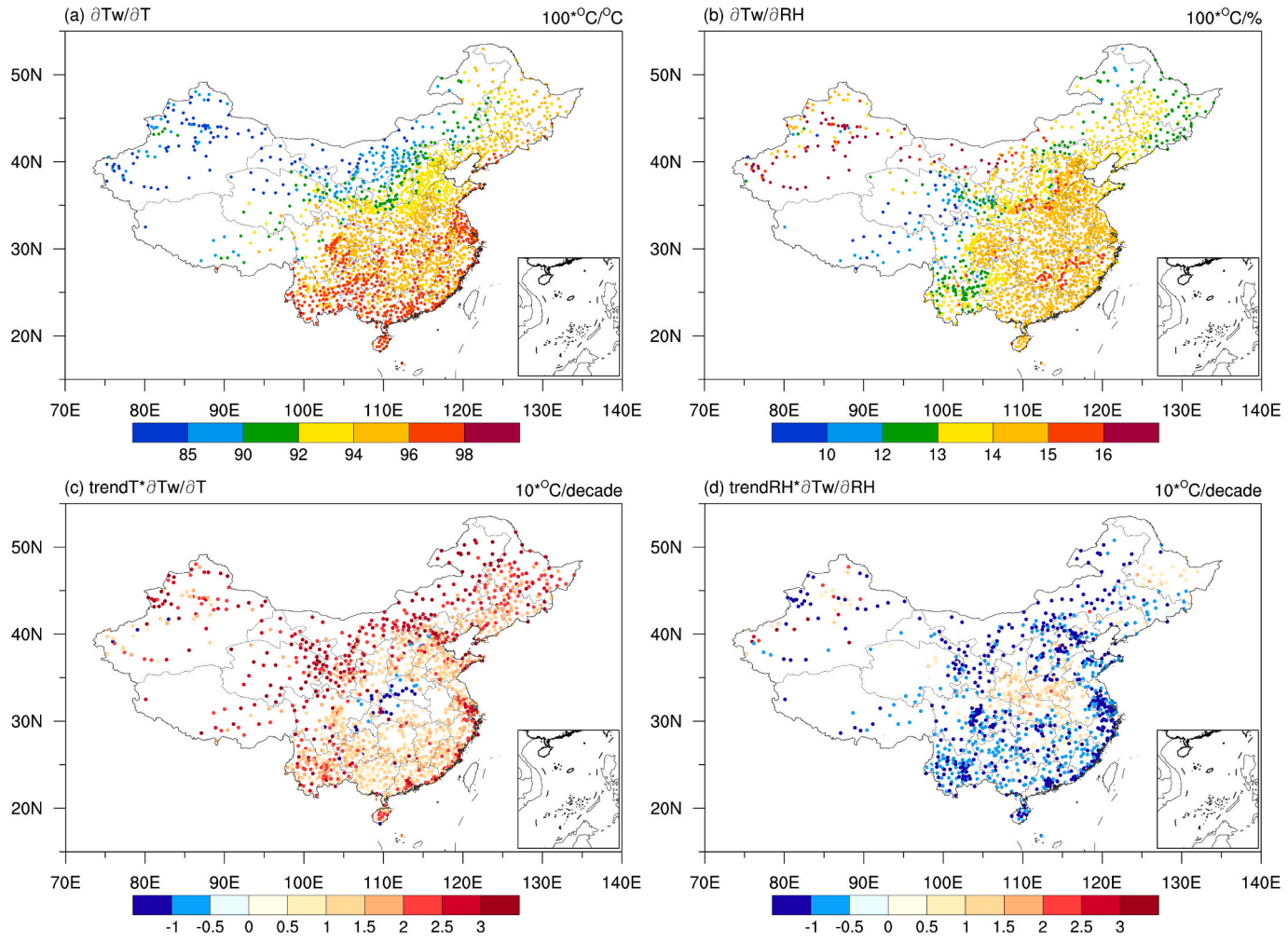


**Fig. 10.** Spatial distributions of the (a) ∂Tw/∂T, (b) ∂Tw/∂RH, (c) trendT*∂Tw/∂T and (d) trendRH*∂Tw/∂RH for 1961–2021. Only stations with significant trend at the 0.1 level are shown in Figure c and d.

from the 1980s in China. It suggests that for the national average, RH has an effect on the variability of WBHWs at decadal scales, whereas temperature mostly drives the long-term trend on the whole.

Time series of temperature-caused and RH-caused HWN components for the three subregions show significant distinction. Among them, the results for South China are more consistent with the national average than the other two regions, especially for the last three decades. In contrast, the temperature-caused component in YRV is dominated by interannual fluctuations and a stable interdecadal period in the last 15 years due to the slowdown of temperature increase. Significantly different are the results for North China, where the time series of temperature-caused component are almost identical to the HWN of WBHWs, with a correlation coefficient of 0.88. Correspondingly, RH-caused HWN component is negligible, with values of less than 1 day for 41 years of the 61 years. This indicates that the change in WBHWs in North China is almost completely controlled by temperature, and RH change contributes little. Additionally, the comparison of Figs. 8c and 11 reveals that when the effect of RH is removed, the time series of temperature-caused component are mostly compatible with the evolution of THWs.

Obviously, the temperature-caused component here refers to the direct effect of temperature, according to the definition in Section 2.3. Due to the climate warming, evaporation and moisture content in air increase, leading to a positive contribution of specific humidity (Fig. S12). The time series is remarkably similar to RH-caused WBHWs, with a more pronounced trend. Correspondingly, the indirect effect of temperature continues to decrease from the 1970s, suppressing the direct effect of temperature. The increasing trend of direct effect exceeds the decreasing trend of indirect effect, making the total effect of temperature increasing. The effects of air pressure in the three subregions remain almost constant. The time series of the components for South China and YRV show a resemblance with the national average. However, the phases of specific humidity in North China is completely opposite to the indirect effect of temperature, resulting in the negligible effect of RH.

The average change in WBHWs for the last 31 year (1991–2021) and contributions of six components were calculated (See Fig. 12 and Table 3). As Fig. 12a indicates, the average change of WBHWs in the past 31 years is remarkably similar to the HWN trends over the period 1961–2021, with a national average of 1.3 days and considerable increase in South China. The warming temperature directly contributes to the positive change of WBHWs over most parts of China (86.3%). At the national level, it induces increase of 2.3 days in WBHWs. The largest direct contribution of temperature is in South China and the eastern coastal areas of YRV, reaching as high as 8 days. This is also the regions where the most significant increase in THWs occurs. Change of temperature in North China also has a pronounced direct effect on WBHWs. The average contribution rates from North China, YRV and South China are 2.0 days, 3.9 days and 7.6 days, respectively (Table 3). On the contrary, change in RH mainly contributes negatively to the variation in WBHWs, with a national average contribution of −0.6 days. Despite having 44.8% positive stations, the majority contributes less than 2 days

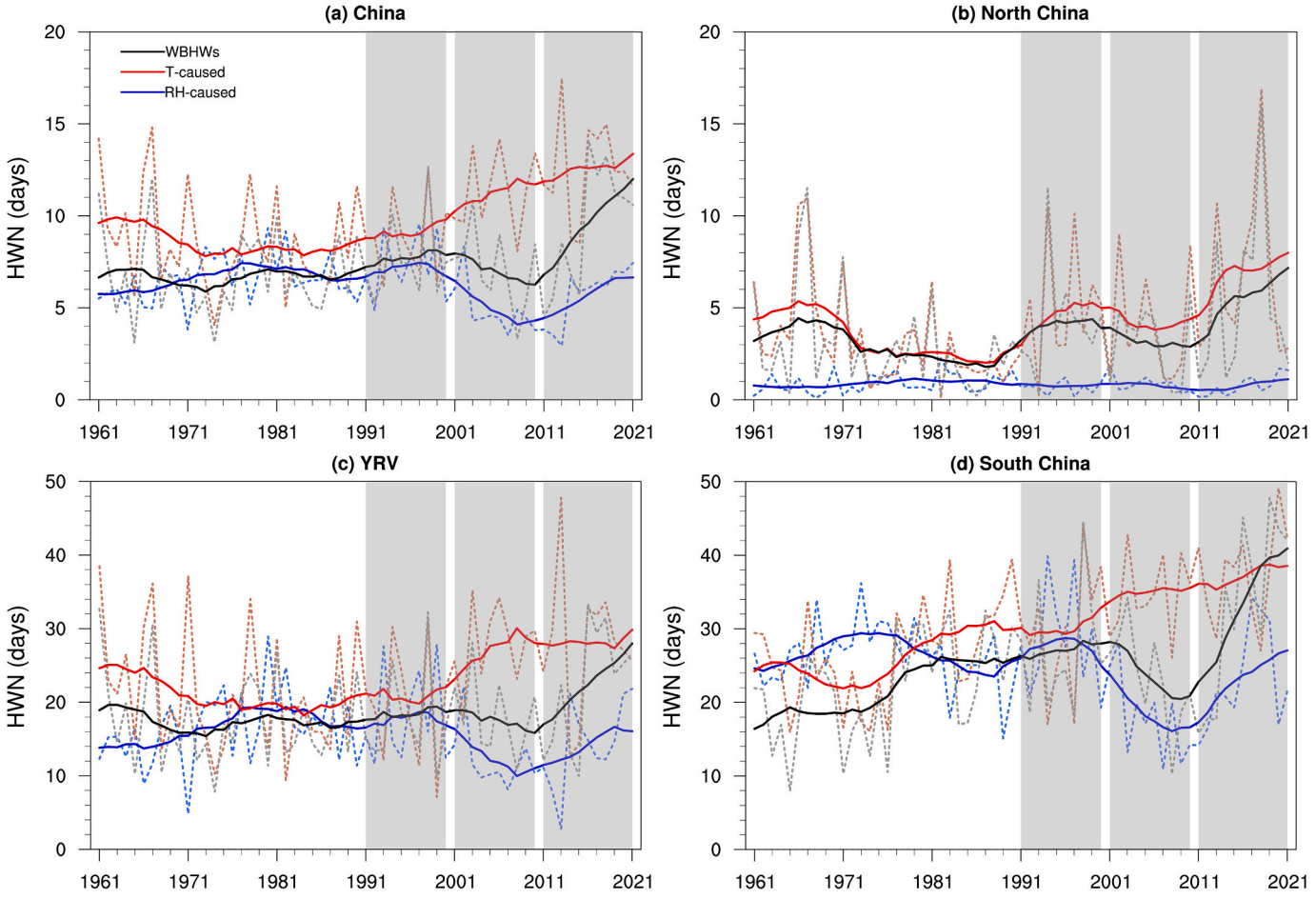


**Fig. 11.** Time series of regional temperature-caused and RH-caused HWN components in China and its three sub-regions during 1961–2021. For comparison, the time series of HWN for WBHWs are also given. The solid lines are the 11-year moving average. The shades represent the three decades of 1991–2000, 2001–2010 and 2011–2021.

to the WBHW change. The most significant negative contributions are located in the lower reaches of YRV and the coastal areas of South China, with a maximum value of more than 8 days. The average contribution of RH in South China (−3.2 days) is mainly due to the indirect effect of temperature (−5.9 days), while specific humidity yields a positive contribution of 4.5 days. The total effect of temperature basically equals that of specific humidity. The negative contribution of RH in YRV, particularly in the lower reaches, is a combined effect of specific humidity and temperature. For the regional average, the indirect effect of temperature (−2.2 days) is obviously larger than the effect of specific humidity (0.7 days). RH changes in North China have a negligible impact, contributing −0.1 days on average. This is consistent with the results in Fig. 11. In addition, the contributions of temperature and RH match well with the trends of HWN based on the two additional Tw (Fig. S13), and the direct effect of temperature is roughly equivalent to the changes in THWs. Note that the combined contribution of temperature and humidity is not equal to the change of WBHWs due to the nonlinearity in the equation of calculating Tw.

## 4. Conclusions and discussion

In this study, the climatology and trends of heatwaves in China as well as the relative contributions of temperature and RH were investigated by using 61-year (1961–2021) observational data. The heatwaves were defined using Tw, an effective metric of combining temperature and humidity, with a unified threshold for the whole of China. It reveals that eastern China experiences the most severe heatwaves, due to the warm and humid conditions. Eastern China was divided into three subregions, namely North China, YRV and South China, and more attentions were paid to these regions. Due to the frequent extreme temperatures, YRV suffers from an average of 19.2 days of THWs per summer, followed by South (15.1 days) and North China (3.7 days). When humidity is concerned, South China experiences more serious WBHWs because of its larger mean Tw and frequent Tw extremes, suffering on 25 days per summer. The fact that WBHWs in South China are more severe than THWs indicates the crucial role of humidity in this region. Since temperature and RH are significantly negatively correlated, WBHWs are highly frequent around the median values of temperature and RH, with higher temperature in YRV and larger RH in North and South China.

As one of the most sensitive areas in the world, China has been suffering significant climate change characterized by warming and drying since the early 20th century (Cheng et al., 2015; Huang et al., 2016). The changes in related climate variables were analyzed, which exhibits an upward trend for summer temperature and Tw during 1961–2021. The warmest regions are located over northern China, which coincides with previous studies (Cheng et al., 2015). Although heatwaves occur in northern China for less than 1 day per summer for the past 61 years, they will become more frequent with substantially rising temperature and Tw. In fact, extreme high temperature events are occurring more often in Northeast China in recent years and will significantly increase in future projections under global warming (Wang et al., 2018; Yang et al., 2021). Due to the significant decreases in the 1990s and the 2000s, RH shows a decreasing trend in most areas.

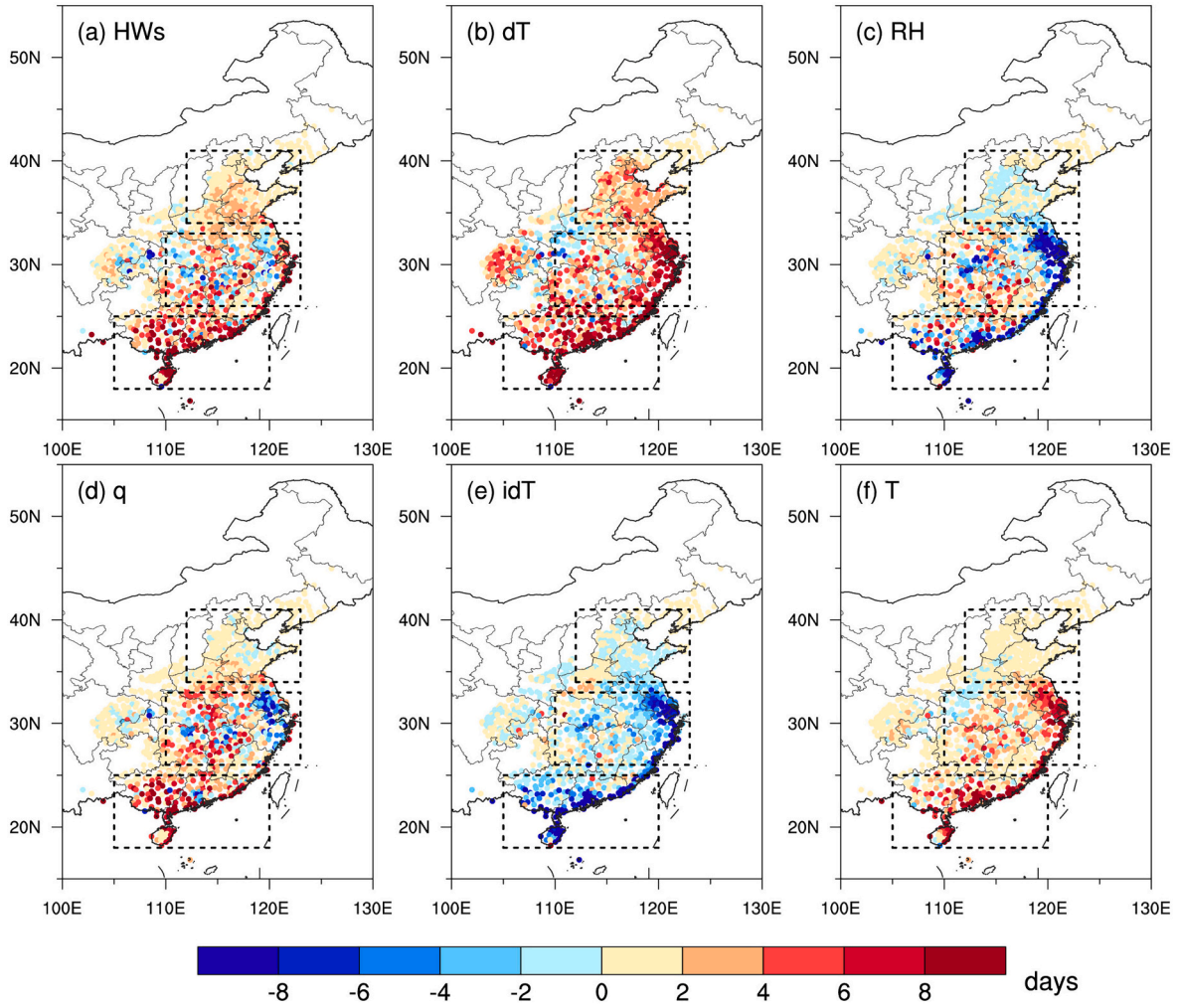


**Fig. 12.** (a) Average change in WBHWs for the period 1991–2021 and contributions of (b) direct effect of temperature, (c) RH, (d) indirect effect of temperature, (e) total effect of temperature, and (f) specific humidity to the change in WBHWs.

**Table 3**
Average changes in THWs and WBHWs for the period 1991–2021 relative to the period 1961–1990 and and contribution rates of direct effect of temperature ($CR_{dT}$), RH ($CR_{RH}$), specific humidity ($CR_q$), indirect effect of temperature ($CR_{idT}$), total effect of temperature ($CR_T$), and air pressure ($CR_P$) to WBHWs in China and its three subregions.

| Index (days) | China | North China | YRV | South China |
|---|---|---|---|---|
| THWs | 2.2 | 2.0 | 3.3 | 7.4 |
| WBHWs | 1.3 | 1.3 | 1.6 | 6.1 |
| $CR_{dT}$ | 2.3 | 2.0 | 3.9 | 7.6 |
| $CR_{RH}$ | −0.6 | −0.1 | −1.6 | −3.2 |
| $CR_q$ | 0.8 | 0.6 | 0.7 | 4.5 |
| $CR_{idT}$ | −1.0 | −0.1 | −2.2 | −5.9 |
| $CR_T$ | 1.1 | 0.2 | 2.6 | 4.7 |
| $CR_P$ | −0.1 | 0.0 | −0.2 | −0.8 |

Affected by the temperature and RH, heatwaves in China are suggested to significantly increase in frequency and intensity, with a nationwide increase of 0.65 and 0.45 days/decade for THWs and WBHWs, respectively. Of these, THWs continues to increase since the early 1970s, while WBHWs have a decadal reduction in the 2000s. The increasing trends are significantly stronger in South China than in the other two regions.

WBHWs in North and South China primarily occur under high humidity, whereas WBHWs in YRV are mainly at extreme temperatures. It indicates the dominant role of humidity on the occurrence of WBHWs in North and South China, while temperature has a major role in YRV. This result may contrast with previous studies, because the threshold in our definition is uniform across the whole country, rather than being a local standard for each station. For example, using local temperature thresholds, Wang et al. (2019) demonstrated that humidity contributes more than temperature to the occurrence of extreme Tw, especially in North and Northwest China. According to $\partial Tw/\partial T$ and $\partial Tw/\partial RH$, Tw is more sensitive to the changes in temperature in the southeast, while in Xinjiang it is more sensitive to the changes in RH. By controlling temperature and RH constant, the effects of RH and temperature on WBHWs were measured. RH has an effect on the variability of WBHWs at decadal scales, but temperature mainly drives the long-term trend on the whole. For the national average, temperature induces an increase in WBHWs of 2.3 days, while RH causes a decrease of −0.6 days. Among the three subregions, South China has the strongest effects of temperature and RH, with contribution rates of 7.6 days and − 3.2 days, respectively. The contribution rates of temperature in North and South China are 2.0 days and 3.9 days, and the contribution of RH are −0.1 days and − 1.6 days, respectively. It means that change in WBHWs in North China is almost completely controlled by temperature. The opposite phases of specific humidity and temperature result in the negligible impact of RH. The negative contribution of RH in South China results from the indirect effect of temperature, whereas in the lower reaches of YRV it is a combination of temperature and specific humidity.

In our study, heatwaves are defined by temperature and Tw, some

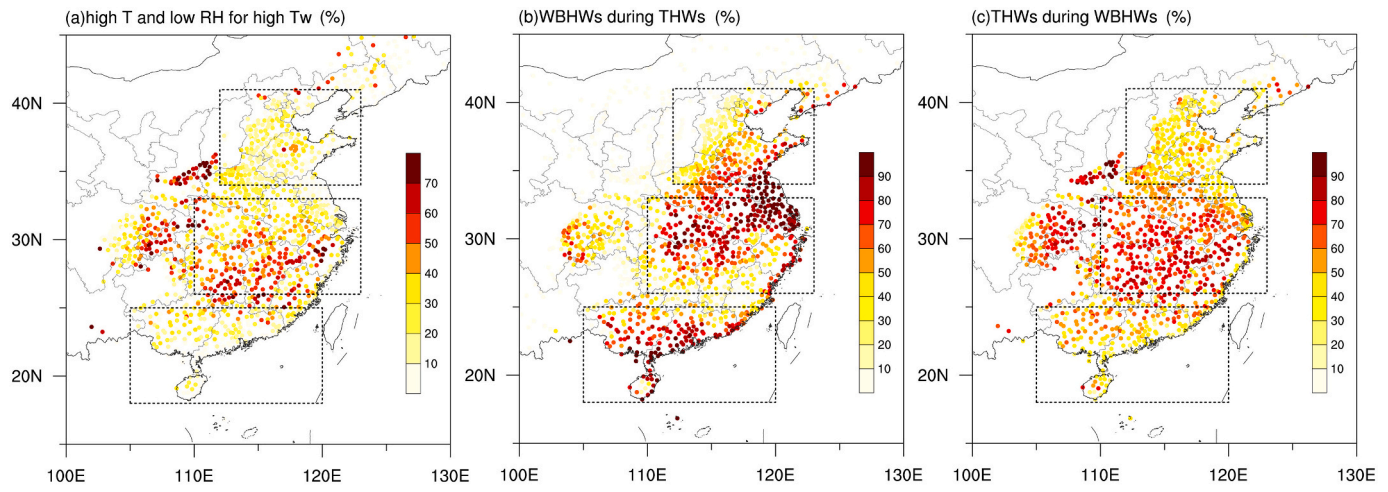


**Fig. 13.** Percentages of (a) high-temperature, low-RH for high Tw, (b) WBHWs during THWs, (c) THWs during WBHWs for the period 1961–2021, where low-RH (high-temperature) means daily RH (temperature) is less (larger) than mean RH (the 90th percentile of temperature) for all summer days during 1961–2021 over the whole China.

other temperature indices and methodologies are also being applied to define heatwaves. Although using apparent temperature generates identical spatial distributions and time series of WBHWs (Fig. S14), it may generate discrepant results based on different indices. Therefore, it indicates the complexity of defining appropriate heatwaves and necessity of comparing multiple methodologies. Some previous studies have addressed this issue. In particular, You et al. (2017) systematically compared the patterns, trends and variations of 16 heatwave indices that were divided into two types using relative and absolute threshold temperatures. It exhibits significant correlations among different indices in the same type and contrasting trends between relative and absolute threshold indices. Even the characteristics of daily maximum, minimum and average temperatures are different. Using maximum temperature generates similar climatological averages and trends of HWN as temperature, while the results based on minimum temperature exhibit large discrepancies, with more apparent increasing trends in eastern China (Fig. S15). Previous studies have shown that minimum temperature increased faster than the maximum temperature in China influenced by the decline of sunshine duration (Shen et al., 2014). It should be noted that we named the heatwaves based on Tw as WBHWs instead of wet heatwaves, as high Tw may be caused by high temperature and low RH. As a result, WBHWs may occur under low RH. Therfore, THWs and WBHWs will co-occur in our definition. As shown in Fig. 13a, at least 10% of the extreme Tw occurs under high-temperature and low-RH conditions at almost all of the stations in eastern China, especially in YRV. The average proportions for North China, YRV and South China are 18.2%, 36.2% and 18.8%, highlighting the critical role of temperature for WBHWs in YRV. Consequently, substantial overlap of THWs and WBHWs exists, with 40.0%, 64.9%, 43.4% WBHWs occurring during THWs, and 40.8%, 64.7%, 43.4 THWs during WBHWs for North China, YRV and South China (Fig. 13c,d). Some studies have classfied heatwaves into dry and wet types based on strict standards (Ha et al., 2022; Luo et al., 2022; Xu et al., 2021). Ding and Ke (2014) defined the dry and wet heat events by a mean RH of 60%, and then investigated their interannual variability. The 60% threshold was also adopted in several other studies (Ge et al., 2021; Xu et al., 2021).

We gave more attention to the three subregions, while the eastern part of the southwest China also has severe heatwaves and has been focused on in some recent studies (Deng et al., 2020; Jiang et al., 2022). Southwest China exhibits more severe THWs than WBHWs in terms of climatological averages and upward trends (Fig. S16). It suffers an average of 7.6 days and 3.9 days of THWs and WBHWs per summer. Changes in WBHWs are dominated by temperature, with contributions of 2.3 days and 0.4 days for temperature and RH, respectively. Additionally, eastern China was divided subjectively according to the characteristics of heatwaves. To obtain more objective classification, cluster analysis or empirical orthogonal function (EOF) decomposition, which can group similar observations into a number of clusters, can be used (Khan and Ahmad, 2004). 90th percentile is chosen as the threshold in this study, and using a relatively higher threshold (e.g., 95th percentile) yields less frequent heatwaves as well as similar primary conclusions. However, heatwaves of various intensities may present distinct characteristics based on alternative methods or indices. For example, Luo and Lau (2019a) found that cautionary heat stress in the North China Plain and parts of central China exhibits more prominent increasing trends, while the strongest trends of danger heat stress mainly appear in middle and lower YRV areas.

The mechanism behind heatwaves is complex, involving factors such as global warming, anomalies in sea surface temperatures (SSTs), atmospheric circulation, local feedbacks and human activities. Previous researchers have revealed that high-pressure anticyclonic systems are favorable circulations for the formation of high temperatures (Freychet et al., 2017; Luo et al., 2020; Tao et al., 2017), which can generate downdrafts and air thermal advection, thus resulting in clear skies and enhanced surface longwave radiation. SSTs can affect the high-pressure system in China through teleconnection. Wei et al. (2023) revealed that the combined impacts of the El Niño–Southern Oscillation (ENSO), Atlantic Multidecadal Oscillation, and Indian Ocean Dipole can explain approximately 60% of the heatwave intensification in China. Using 13 high-skill climate models, Chen and Zhou (2018) showed that approximately 2/3 of the heatwave variability in YRV can be attributed to SSTs, with one-half of the influence coming from ENSO. During the summers following El Niño, a stronger northwestern Pacific subtropical high was observed, which is favorable for more heatwaves over eastern China (Luo and Lau, 2019b). This correlation is more pronounced during positive phases of the Pacific Decadal Oscillation (Liu et al., 2019). Such influences of ENSO are particularly strong in southern China, whereas heatwaves in northern China are closely associated with the North Atlantic Ocean (Deng et al., 2019; Lu et al., 2020; Luo and Lau, 2019a). In addition, local feedbacks, including urbanization, have an important influence on the development of heatwaves. A recent study suggested that 9%–20% of the heatwaves in Eastern China in 2022 are caused by SSTs, and local soil moisture–temperature feedback accounts for 42%–66% (Jiang et al., 2023). Urbanization is also one major drivers of heatwaves in cities, which contributes to 30–50% of hot extremes in China (Kong et al., 2020; Wang et al., 2021; Wu et al., 2020). The contribution of urbanization is stronger in wet climates, reaching 50% in the Pearl River delta region (Liao et al., 2018; Luo and Lau, 2017).

Nevertheless, the interaction of temperature and humidity makes the mechanisms of WBHWs complex. Wet heatwaves are also associated with the eastward extension of the South Asian high, the westward extension of the western North Pacific subtropical high, and low-level anticyclonic anomalies (Luo et al., 2022). Ha et al. (2022) revealed that dry heatwaves are caused by adiabatic heating under the influence of the convergence of anomalous wave activity flux over northern East Asia, while wet heatwaves are triggered by the locally generated anticyclonic anomalies and amplified by cloud and water vapor feedback. The increased water vapor during wet heatwaves in the Middle and Lower Reaches of the Yellow River is brought by the Western Pacific subtropical High from the low-latitude oceans (Ge et al., 2021). In our future works, it is of interests to compare the dry and wet heatwaves in China and explore the mechanism in different subregions.

## CRediT authorship contribution statement

**Shanjun Cheng:** Formal analysis, Methodology, Writing – original draft, Writing – review & editing. **Shanshan Wang:** Conceptualization, Methodology, Writing – review & editing. **Mingcai Li:** Conceptualization. **Yongli He:** Methodology, Validation.

## Declaration of competing interest

The authors declare that they have no known competing financial interests or personal relationships that could have appeared to influence the work reported in this paper.

## Data availability

Datasets related to this article can be found at http://data.cma.cn, provided by the China Meteorological Administration.

## Acknowledgments

This work was supported by the National Natural Science Foundation of China (Grant numbers 42075018, 41805058); and the Open Project of Lanzhou Institute of Arid Meteorology CMA (Grant number IAM202203).

## Appendix A. Supplementary data

Supplementary data to this article can be found online at https://doi.org/10.1016/j.atmosres.2024.107366.

## References

Chen, X., Zhou, T., 2018. Relative contributions of external SST forcing and internal atmospheric variability to July-August heat waves over the Yangtze River valley. Clim. Dyn. 51, 4403–4419. https://doi.org/10.1007/s00382-017-3871-y.

Cheng, S., Guan, X., Huang, J., Ji, F., Guo, R., 2015. Long-term trend and variability of soil moisture over East Asia. J. Geophys. Res. Atmos. 120 (17), 8658–8670. https://doi.org/10.1002/2015JD023206.

Deng, K., Yang, S., Ting, M., Zhao, P., Wang, Z., 2019. Dominant modes of China summer heat waves driven by global sea surface temperature and atmospheric internal variability. J. Clim. 32 (12), 3761–3775. https://doi.org/10.1175/JCLI-D-18-0256.1.

Deng, K., Jiang, X., Hu, C., Chen, D., 2020. More frequent summer heat waves in southwestern China linked to the recent declining of Arctic Sea ice. Environ. Res. Lett. 15 (7), 074011 https://doi.org/10.1088/1748-9326/ab8335.

Ding, T., Ke, Z., 2014. Characteristics and changes of regional wet and dry heat wave events in China during 1960–2013. Theor. Appl. Climatol. 122, 651–665. https://doi.org/10.1007/s00704-014-1322-9.

Ding, T., Qian, W., 2011. Geographical patterns and temporal variations of regional dry and wet heatwave events in China during 1960–2008. Adv. Atmos. Sci. 28, 322–337. https://doi.org/10.1007/s00376-010-9236-7.

Freychet, N., Tett, S., Wang, J., Hegerl, G., 2017. Summer heat waves over eastern China: dynamical processes and trend attribution. Environ. Res. Lett. 12 (2), 024015 https://doi.org/10.1088/1748-9326/aa5ba3.

Ge, H., Zeng, G., Iyakaremye, V., Yang, X., Wang, Z., 2021. Comparison of atmospheric circulation anomalies between dry and wet extreme high-temperature days in the middle and lower reaches of the Yellow river. Atmosphere 12 (10), 1265. https://doi.org/10.3390/atmos12101265.

Ha, K.J., Seo, Y.W., Yeo, J.H., Timmermann, A., Chung, E.S., Franzke, C.L., et al., 2022. Dynamics and characteristics of dry and moist heatwaves over East Asia. NPJ Clim. Atmos. Sci. 5 (1), 49. https://doi.org/10.1038/s41612-022-00272-4.

Hao, L., Huang, X., Qin, M., Liu, Y., Li, W., Sun, G., 2018. Ecohydrological processes explain urban dry island effects in a wet region, southern China. Water Resour. Res. 54 (9), 6757–6771. https://doi.org/10.1029/2018WR023002.

Hao, Z., Chen, Y., Feng, S., Liao, Z., An, N., Li, P., 2023. The 2022 Sichuan-Chongqing spatio-temporally compound extremes: a bitter taste of novel hazards. Sci. Bull. https://doi.org/10.1016/j.scib.2023.05.034. S2095-9273, 00367.

Heo, S., Bell, M., Lee, T., 2019. Comparison of health risks by heat wave definition: applicability of wet-bulb globe temperature for heat wave criteria. Environ. Res. 168, 158–170. https://doi.org/10.1016/j.envres.2018.09.032.

Hu, L., Huang, G., Qu, X., 2017. Spatial and temporal features of summer extreme temperature over China during 1960–2013. Theor. Appl. Climatol. 128 (3), 821–833. https://doi.org/10.1007/s00704-016-1741-x.

Huang, J., Ji, M., Xie, Y., Wang, S., He, Y., Ran, J., 2016. Global semi-arid climate change over last 60 years. Clim. Dyn. 46 (3), 1131–1150. https://doi.org/10.1007/s00382-015-2636-8.

Jiang, L., Chen, Y.D., Li, J., Liu, C., 2022. Amplification of soil moisture deficit and high temperature in a drought-heatwave co-occurrence in southwestern China. Nat. Hazards 111 (1), 641–660. https://doi.org/10.1007/s11069-021-05071-3.

Jiang, J., Liu, Y., Mao, J., Wu, G., 2023. Extreme heatwave over Eastern China in summer 2022: the role of three oceans and local soil moisture feedback. Environ. Res. Lett. 18 (4), 044025 https://doi.org/10.1088/1748-9326/acc5fb.

Jones, B., O'Neill, B.C., McDaniel, L., McGinnis, S., Mearns, L.O., Tebaldi, C., 2015. Future population exposure to US heat extremes. Nat. Clim. Chang. 5 (7), 652–655. https://doi.org/10.1038/nclimate2631.

Kang, S., Eltahir, E.A., 2018. North China Plain threatened by deadly heatwaves due to climate change and irrigation. Nat. Commun. 9 (1), 1–9. https://doi.org/10.1038/s41467-018-05252-y.

Khan, S.S., Ahmad, A., 2004. Cluster center initialization algorithm for K-means clustering. Pattern Recogn. Lett. 25 (11), 1293–1302. https://doi.org/10.1016/j.patrec.2004.04.007.

Kong, D., Gu, X., Li, J., Ren, G., Liu, J., 2020. Contributions of global warming and urbanization to the intensification of human- perceived heatwaves over China. J. Geophys. Res. Atmos. 125 (18) https://doi.org/10.1029/2019JD032175 e2019JD032175.

Kumaraswamy, P., 1980. A generalized probability density function for double-bounded random processes. J. Hydrol. 46 (1–2), 79–88. https://doi.org/10.1016/0022-1694(80)90036-0.

Li, Q., Dong, W., 2009. Detection and adjustment of undocumented discontinuities in Chinese temperature series using a composite approach. Adv. Atmos. Sci. 26 (1), 143–153. https://doi.org/10.1007/s00376-009-0143-8.

Li, Q., Liu, X., Zhang, H., Peterson, T.C., Easterling, D.R., 2004. Detecting and adjusting temporal inhomogeneity in Chinese mean surface air temperature data. Adv. Atmos. Sci. 21 (2), 260–268. https://doi.org/10.1007/BF02915712.

Li, X., Ren, G., Wang, S., You, Q., Sun, Y., Ma, Y., et al., 2021. Change in the heatwave statistical characteristics over China during the climate warming slowdown. Atmos. Res. 247, 105152 https://doi.org/10.1016/j.atmosres.2020.105152.

Liao, W., Liu, X., Li, D., Luo, M., Wang, D., Wang, S., et al., 2018. Stronger contributions of urbanization to heat wave trends in wet climates. Geophys. Res. Lett. 45, 11310–11317. https://doi.org/10.1029/2018GL079679.

Lin, Q., Yuan, J., 2022. Linkages between amplified quasi-stationary waves and humid heat extremes in northern hemisphere midlatitudes. J. Clim. 35 (24), 4645–4658. https://doi.org/10.1175/JCLI-D-21-0952.1.

Liu, Q., Zhou, T., Mao, H., Fu, C., 2019. Decadal variations in the relationship between the western Pacific subtropical high and summer heat waves in East China. J. Clim. 32 (5), 1627–1640. https://doi.org/10.1175/JCLI-D-18-0093.1.

Lu, C., Ye, J., Wang, S., Yang, M., Li, Q., He, W., et al., 2020. An unusual heat wave in North China during midsummer, 2018. Front. Earth Sci. 8, 238. https://doi.org/10.3389/feart.2020.00238.

Luo, M., Lau, N.C., 2017. Heat waves in southern China: synoptic behavior, long-term change, and urbanization effects. J. Clim. 30 (2), 703–720. https://doi.org/10.1175/JCLI-D-16-0269.1.

Luo, M., Lau, N.C., 2018. Increasing heat stress in urban areas of eastern China: acceleration by urbanization. Geophys. Res. Lett. 45 (23), 13060–13069. https://doi.org/10.1029/2018GL080306.

Luo, M., Lau, N.C., 2019a. Characteristics of summer heat stress in China during 1979–2014: climatology and long-term trends. Clim. Dyn. 53 (9), 5375–5388. https://doi.org/10.1007/s00382-019-04871-5.

Luo, M., Lau, N.C., 2019b. Amplifying effect of ENSO on heat waves in China. Clim. Dyn. 52 (5–6), 3277–3289. https://doi.org/10.1007/s00382-018-4322-0.

Luo, M., Ning, G., Xu, F., Wang, S., Liu, Z., Yang, Y., 2020. Observed heatwave changes in arid Northwest China: physical mechanism and long-term trend. Atmos. Res. 242, 105009 https://doi.org/10.1016/j.atmosres.2020.105009.

Luo, M., Wu, S., Liu, Z., Lau, N.C., 2022. Contrasting circulation patterns of dry and humid heatwaves over southern China. Geophys. Res. Lett. 49 (16) https://doi.org/10.1029/2022GL099243 e2022GL099243.

Ma, F., Yuan, X., 2023. When will the unprecedented 2022 summer heat waves in Yangtze River basin become normal in a warming climate? Geophys. Res. Lett. 50 (4) https://doi.org/10.1029/2022GL101946 e2022GL101946.

Meehl, G.A., Tebaldi, C., 2004. More intense, more frequent, and longer lasting heat waves in the 21st century. Science 305 (5686), 994–997. https://doi.org/10.1126/science.1098704.

Mora, C., Dousset, B., Caldwell, I.R., Powell, F.E., Geronimo, R.C., Bielecki, C.R., et al., 2017. Global risk of deadly heat. Nat. Clim. Chang. 7 (7), 501–506. https://doi.org/10.1038/nclimate3322.

Ning, G., Luo, M., Wang, S., Liu, Z., Wang, P., Yang, Y., 2022. Dominant modes of summer wet bulb temperature in China. Clim. Dyn. 59, 1488–1743. https://doi.org/10.1007/s00382-021-06051-w.

Niu, Z., Wang, L., Fang, L., Li, J., Yao, R., 2020. Spatiotemporal variations in monthly relative humidity in China based on observations and CMIP5 models. Int. J. Climatol. 40 (15), 6382–6395. https://doi.org/10.1002/joc.6587.

Peng, J.B., 2014. An investigation of the formation of the heat wave in southern China in summer 2013 and the relevant abnormal subtropical high activities. Atmos. Ocean. Sci. Lett. 7 (4), 286–290. https://doi.org/10.3878/j.issn.1674-2834.13.0097.

Perkins, S.E., Alexander, L.V., 2013. On the measurement of heat waves. J. Clim. 26 (13), 4500–4517. https://doi.org/10.1175/JCLI-D-12-00383.1.

Perkins, S.E., Alexander, L.V., Nairn, J., 2012. Increasing frequency, intensity and duration of observed global heatwaves and warm spells. Geophys. Res. Lett. 39 (20), L20714. https://doi.org/10.1029/2012GL053361.

Qian, C., Yan, Z., Wu, Z., Fu, C., Tu, K., 2011. Trends in temperature extremes in association with weather-intraseasonal fluctuations in eastern China. Adv. Atmos. Sci. 28 (2), 297–309. https://doi.org/10.1007/s00376-010-9242-9.

Qian, C., Ye, Y., Jiang, J., Zhong, Y., Zhang, Y., Pinto, I., et al., 2024. Rapid attribution of the record-breaking heatwave event in North China in June 2023 and future risks. Environ. Res. Lett. 19 (1), 014028 https://doi.org/10.1088/1748-9326/ad0dd9.

Raymond, C., Singh, D., Horton, R., 2017. Spatiotemporal patterns and synoptics of extreme wet-bulb temperature in the contiguous United States. J. Geophys. Res. Atmos. 122 (24), 13108–13124. https://doi.org/10.1002/2017JD027140.

Russo, S., Sillmann, J., Sterl, A., 2017. Humid heat waves at different warming levels. Sci. Rep. 7 (1), 1–7. https://doi.org/10.1038/s41598-017-07536-7.

Shen, X., Liu, B., Li, G., Wu, Z., Jin, Y., Yu, P., Zhou, D., 2014. Spatiotemporal change of diurnal temperature range and its relationship with sunshine duration and precipitation in China. J. Geophys. Res.-Atmos. 119 (23), 13163–13179. https://doi.org/10.1002/2014JD022326.

Smoyer-Tomic, K.E., Kuhn, R., Hudson, A., 2003. Heat wave hazards: an overview of heat wave impacts in Canada. Nat. Hazards 28, 465–486. https://doi.org/10.1023/A:1022946528157.

Stull, R., 2011. Wet-bulb temperature from relative humidity and air temperature. J. Appl. Meteorol. Climatol. 50 (11), 2267–2269. https://doi.org/10.1175/JAMC-D-11-0143.1.

Sun, X., Sun, Q., Zhou, X., Li, X., Yang, M., Yu, A., Geng, F., 2014a. Heat wave impact on mortality in Pudong New Area, China in 2013. Sci. Total Environ. 493, 789–794. https://doi.org/10.1016/j.scitotenv.2014.06.042.

Sun, Y., Zhang, X., Zwiers, F.W., Song, L., Wan, H., Hu, T., et al., 2014b. Rapid increase in the risk of extreme summer heat in Eastern China. Nat. Clim. Chang. 4 (12), 1082–1085. https://doi.org/10.1038/nclimate2410.

Tao, P., Zhang, Y., 2019. Large-scale circulation features associated with the heat wave over Northeast China in summer 2018. Atmos. Ocean. Sci. Lett. 12 (4), 254–260. https://doi.org/10.1080/16742834.2019.1610326.

Tao, H., Fischer, T., Su, B., Mao, W., Jiang, T., Fraedrich, K., 2017. Observed changes in maximum and minimum temperatures in Xinjiang autonomous region, China. Int. J. Climatol. 37 (15), 5120–5128. https://doi.org/10.1002/joc.5149.

Wang, J., Yan, Z., 2021. Rapid rises in the magnitude and risk of extreme regional heat wave events in China. Weather Clim. Extrem. 34, 100379 https://doi.org/10.1016/j.wace.2021.100379.

Wang, L., Wang, W.J., Wu, Z., Du, H., Shen, X., Ma, S., 2018. Spatial and temporal variations of summer hot days and heat waves and their relationships with large-scale atmospheric circulations across Northeast China. Int. J. Climatol. 38 (15), 5633–5645. https://doi.org/10.1002/joc.5768.

Wang, P., Leung, L.R., Lu, J., Song, F., Tang, J., 2019. Extreme wet-bulb temperatures in China: the significant role of moisture. J. Geophys. Res. Atmos. 124 (22), 11944–11960. https://doi.org/10.1029/2019JD031477.

Wang, J., Chen, Y., Tett, S.F., Yan, Z., Zhai, P., Feng, J., Xia, J., 2020. Anthropogenically-driven increases in the risks of summertime compound hot extremes. Nat. Commun. 11 (1), 528. https://doi.org/10.1038/s41467-019-14233-8.

Wang, J., Chen, Y., Liao, W., He, G., Tett, S.F., Yan, Z., et al., 2021. Anthropogenic emissions and urbanization increase risk of compound hot extremes in cities. Nat. Clim. Chang. 11 (12), 1084–1089. https://doi.org/10.1038/s41558-021-01196-2.

Wei, K., Chen, W., 2009. Climatology and trends of high temperature extremes across China in summer. Atmos. Ocean. Sci. Lett. 2 (3), 153–158. https://doi.org/10.1080/16742834.2009.11446795.

Wei, K., Chen, W., 2011. An abrupt increase in the summer high temperature extreme days across China in the mid-1990s. Adv. Atmos. Sci. 28 (5), 1023–1029. https://doi.org/10.1007/s00376-010-0080-6.

Wei, J., Han, W., Wang, W., Zhang, L., Rajagopalan, B., 2023. Intensification of heatwaves in China in recent decades: roles of climate modes. NPJ Clim. Atmos. Sci. 6 (1), 98. https://doi.org/10.1038/s41612-023-00428-w.

Wu, X., Wang, L., Yao, R., Luo, M., Wang, S., Wang, L., 2020. Quantitatively evaluating the effect of urbanization on heat waves in China. Sci. Total Environ. 731, 138857 https://doi.org/10.1016/j.scitotenv.2020.138857.

Xu, F., Chan, T.O., Luo, M., 2021. Different changes in dry and humid heat waves over China. Int. J. Climatol. 41 (2), 1369–1382. https://doi.org/10.1002/joc.6815.

Yang, X., Zeng, G., Zhang, G., Li, J., Li, Z., Hao, Z., 2021. Interdecadal variations of different types of summer heat waves in Northeast China associated with AMO and PDO. J. Clim. 34 (19), 7783–7797. https://doi.org/10.1175/JCLI-D-20-0939.1.

Yao, R., Hu, Y., Sun, P., Bian, Y., Liu, R., Zhang, S., 2022. Effects of urbanization on heat waves based on the wet-bulb temperature in the Yangtze River Delta urban agglomeration, China. Urban Clim. 41, 101067 https://doi.org/10.1016/j.uclim.2021.101067.

You, Q., Jiang, Z., Kong, L., Wu, Z., Bao, Y., Kang, S., Pepin, N., 2017. A comparison of heat wave climatologies and trends in China based on multiple definitions. Clim. Dyn. 48 (11), 3975–3989. https://doi.org/10.1007/s00382-016-3315-0.

Yu, S., Tett, S.F., Freychet, N., Yan, Z., 2021. Changes in regional wet heatwave in Eurasia during summer (1979–2017). Environ. Res. Lett. 16 (6), 064094 https://doi.org/10.1088/1748-9326/ac0745.

Yuan, J., Stein, M.L., Kopp, R.E., 2020. The evolving distribution of relative humidity conditional upon daily maximum temperature in a warming climate. J. Geophys. Res. Atmos. 125 (19) https://doi.org/10.1029/2019JD032100 e2019JD032100.

Zhou, C., Wang, K., Qi, D., Tan, J., 2019. Attribution of a record-breaking heatwave event in summer 2017 over the Yangtze river delta. Bull. Am. Meteorol. Soc. 100 (1), S97–S103. https://doi.org/10.1175/BAMS-D-18-0134.1.